Electronic Supplementary Information (ESI)

Development and application of redox-active cyclometallating ligands based on W(II) alkyne complexes

Mareike Hüttenschmidt,[a] Helge Lange,[a] Miguel Andre Argüello Cordero,[c] Alexander Villinger,[a] Stefan Lochbrunner[c] and Wolfram W. Seidel*[a,b]

[a] Institut für Chemie, Universität Rostock, 18055 Rostock, Germany; wolfram.seidel@uni-rostock.de

[b] Leibniz Institut für Katalyse e.V., 18059 Rostock.

[c] Institut für Physik, Universität Rostock, 18055 Rostock, Germany; stephan.lochbrunner@uni-rostock.de

Content

1. Crystallographic details

1.1 Overview

Single crystals suitable for X-ray diffraction analysis were selected in Fomblin YR-1800 perfluoropolyether oil (Alfa Aesar) at ambient temperature and mounted on a glass fiber. During the measurement, the samples were cooled to 123(2) K. Diffraction data were collected on a Bruker D8 QUEST diffractometer and a Bruker Kappa Apex II diffractometer using graphite monochromated Mo-K_α radiation. Structure solutions were found by direct methods (SHELXS-97 or SHELXS-2013)[1] and were refined by full-matrix least-squares procedures on F^2 (SHELXL-2013)[2]. All non-hydrogen atoms were anisotropically refined unless stated otherwise. Hydrogen atoms were included at calculated positions with fixed thermal parameters unless stated otherwise. The unit cell of **5**-PF_6 contains seven dichloromethane molecules and the unit cell of **6** contains eight dichloromethane molecules, which have been treated as a diffuse contribution to the overall scattering without specific atom positions by SQUEEZE/PLATON.

Table S1. Crystallographic details for **1**, **2**, *like*-**5** and 0.77 $Ru(dppp)_2Cl$·0.23 $Ru(dppp)_2Cl_2$.

	1	**2**	*like*-**5**	$Ru(dppp)_2Cl$
empirical formula	$C_{34}H_{41}BIN_6OPW$· 0.3 CH_2Cl_2·0.5 C_5H_{12}	$C_{27}H_{35}BBrN_7OW$	$C_{68}H_{80}Au_2B_2I_2N_{12}O_2P_2W_2$· 2.89 CH_2Cl_2	0.77 $C_{54}H_{52}ClP_4Ru$· 0.23 $C_{54}H_{52}Cl_2P_4Ru$· 0.89 C_4H_8O
M /g·mol^{-1}	964.06	748,19	2440.62	1033.77
colour, habit	green, block	green, block	green, block	yellow, block
crystal system	monoclinic	monoclinic	triclinic	monoclinic
space group	C 2/c	P 2_1/n	P-1	P 21/n
a / Å	44.299(16)	9.8840(6)	10.9589(9)	13.1304(9)
b / Å	10.596(4)	15.1727 (10)	11.3595(9)	10.5290(7)
c / Å	16.986(6)	19.1312 (12)	32.950(3)	35.658(2)
α / °	90	90	97.652(3)	90
β / °	102.482(12)	96.075	93.120(3)	100.466(2)
γ / °	90	90	92.069(3)	90
V / Å^3	7785(5)	2852.9 (3)	4055.5(6)	4847.7(6)
Z	8	4	2	4
ρ_{calcd} / g·cm^{-3}	1.645	1.742	1.999	1.416
μ / mm^{-3}	3.881	5.48	7.475	0.564
measured refl.	83830	59214	205863	106999
unique refl.	14069	8305	28133	14139
refl. with $I > 2\sigma(I)$	10616	6023	20310	11797
R_{int}	0.0709	0.081	0.0990	0.0606
parameter/restraints	466/24	353/0	981/109	681/239
R_1 [$I > 2\sigma(I)$]	0.0527	0.0385	0.0458	0.0522
wR_2 (all data)	0.1465	0.0669	0.1004	0.1062
GooF	1.101	1.058	1.033	1.196
Resid. density [eÅ^{-3}]	3.691/-2.094	1.915/ -1.672	2.190/-2.071	1.215/-1.311
CCDC	2093320	2093319	2093322	2093321

Table S 2. Crystallographic details for *unlike*-**5**, **6**-PF_6 and **7**.

	unlike-**5**	**6**-PF_6	**7**
empirical formula	$C_{68}H_{80}Au_2B_2I_2N_{12}O_2P_2W_2$· 2 C_4H_8O	$C_{47}H_{50}BBrF_6N_{11}OPRuW$· 1.375 CH_2Cl_2	$C_{49}H_{50}BBrIrN_9OW$· 4 CH_2Cl_2
M /g·mol^{-1}	2340.64	1422.36	1587.45
colour, habit	green, block	black, needle	orange, needle
crystal system	triclinic	orthorhombic	triclinic
space group	P-1	Pbcn	P-1
a / Å	10.9377(5)	30.5669(19)	10.103(2)
b / Å	11.2089(6)	18.0426(12)	16.208(4)
c / Å	16.0538(8)	19.5693(10)	18.094(4)
α / °	84.307(2)	90	85.391(6)
β / °	83.450(2)	90	75.116(5)
γ / °	87.264(2)	90	75.734(5)
V / Å^3	1944.38(17)	10792.6(11)	2774.7(10)
Z	1	8	2
ρ_{calcd} / g·cm^{-3}	1.999	1.751	1.900
μ / mm^{-3}	7.601	3.385	5.621
measured refl.	60412	366456	63910
unique refl.	13498	13019	12082
refl. with $I > 2\sigma(I)$	11322	11322	7632
R_{int}	0.0330	0.0840	0.1275
parameter/restraints	469/0	726/375	577/0
R_1 [$I > 2\sigma(I)$]	0.0349	0.0479	0.0630
wR_2 (all data)	0.0792	0.0743	0.1517
GooF	1.221	1.161	0.962
Resid. density [eÅ^{-3}]	4.715/-2.779	1.063 /-1.168	3.557/ -3.429
CCDC	–	2093324	2093323

1.2 Molecular structures of **1**, **2**, [**3**]$_2$ and 0.77 Ru(dppp)$_2$Cl·0.23 Ru(dppp)$_2$Cl$_2$

Molecular structure of 1

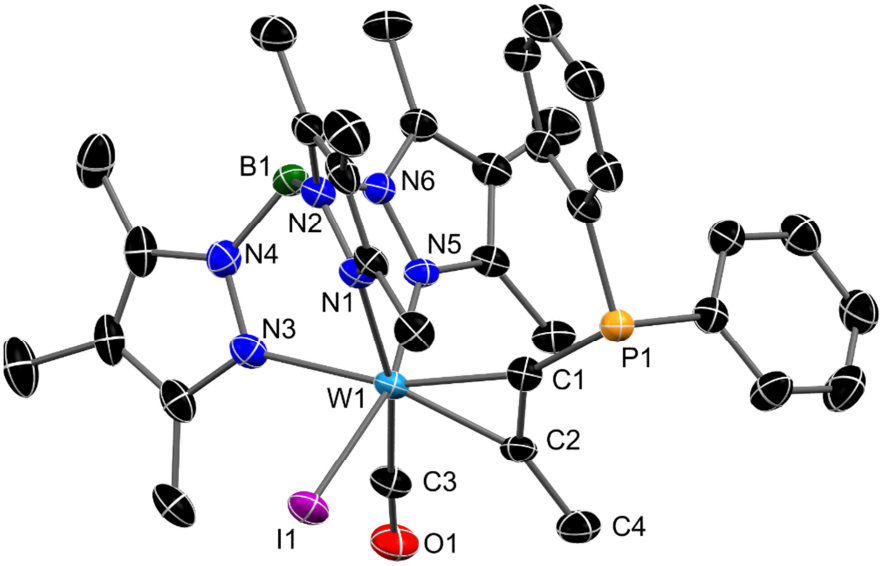

Figure S1. Molecular structure of **1** in the crystal of **1** 0.3 CH_2Cl_2·0.5 C_5H_{12}. Thermal ellipsoids are drawn at 50 % probability. Co-crystallized dichloromethane, *n*-pentane and hydrogen atoms have been omitted for clarity. Selected bond lengths [Å] and angles [°]: W1–C1 2.043(6), W1–C2 2.048(6), W1–C3 1.944(7), W1–I1 2.8045(8), W1–N1 2.255(5), W1–N3 2.231(6), W1–N5 2.183(5), C1–C2 1.339(9), C1–P1 1.784(6), C2-C4 1.483(9), C2–C1–P1 133.3(5), C1-C2-C4 138.6(6).

Molecular structure of 2

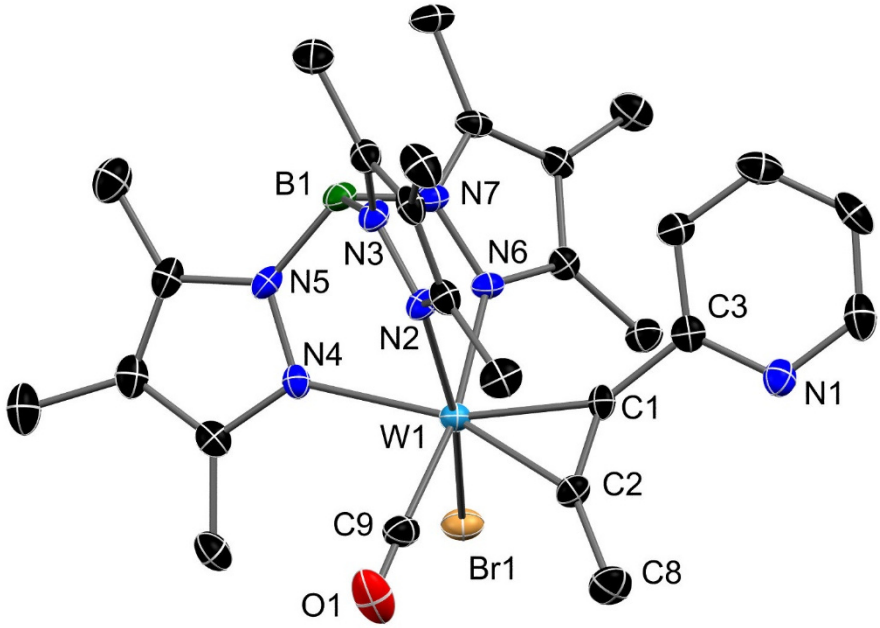

Figure S2. Molecular structure of **2** in the crystal. Thermal ellipsoids are drawn at 50 % probability. Hydrogen atoms have been omitted for clarity. Selected bond lengths [Å] and angles [°]: W1–C1 2.023(4), W1–C2 2.062(4), W1–C9 1.963(5), W1–Br1 2.5857(5), W1–N2 2.174(3),W1–N4 2.220(3), W1–N6 2.226(3), C1–C2 1.297(6), C1–C3 1.460(6), C2-C8 1.482(6), C2–C1–C3 141.4(4), C1-C2-C8 142.7(4).

Molecular structure of $[3]_2$

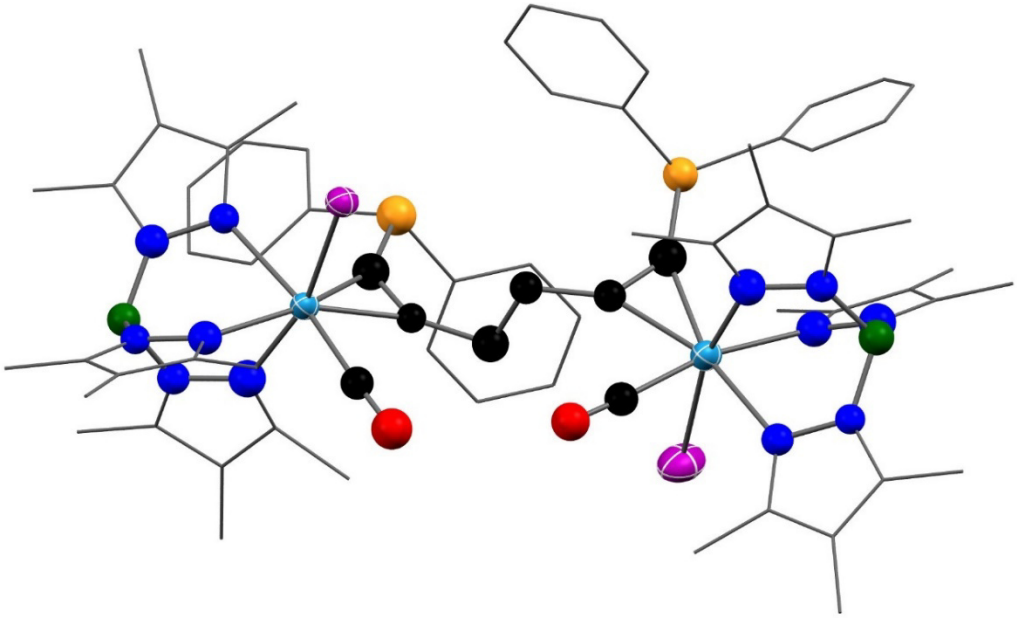

Figure S3. Molecular structure of $(\mathbf{3})_2$. Thermal ellipsoids are drawn at 50 % probability. Hydrogen atoms have been omitted for clarity. The carbon atoms of Tp* and phenyl groups are displayed as wireframe.

Molecular structure of 0.77 $Ru(dppp)_2Cl$·0.23 $Ru(dppp)_2Cl_2$

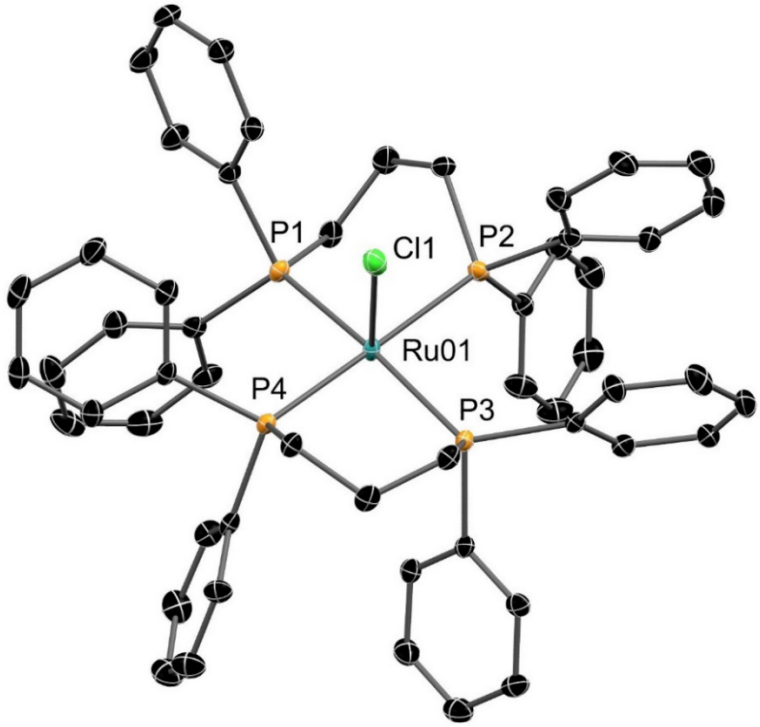

Figure S4. Molecular structure of $Ru(dppp)_2Cl$ in the crystal of 0.77 $C_{54}H_{52}ClP_4Ru$·0.23 $C_{54}H_{52}Cl_2P_4Ru$·0.89 C_4H_8O. Thermal ellipsoids are drawn at 50 % probability. Co-crystallized *n*-pentane and hydrogen atoms have been omitted for clarity. Selected bond lengths [Å] and angles [°]: Ru01-Cl1 2.5497(8), Ru01-Cl2 2.516(3), Ru01-P3 2.3386(7), Ru01-P2 2.3841(8), Ru01-P4 2.3843(7), Ru01-P1 2.3856(7), P4-Ru01-P3 87.19(2), P3-Ru01-P2 92.12(3), P2-Ru01-P4 176.72(3).

2. Experimental section

2.1 General information

All operations were carried out in an atmosphere of dry argon using Schlenk and glove box techniques. Solvents for reactions were dried and saturated with argon by standard methods and freshly distilled prior to use. Solvents for chromatography were used as purchased from commercial sources. NMR spectra were recorded at 298 or 300 K using Bruker Avance 250, 300 or 500 MHz spectrometers. In ^{1}H and ^{13}C NMR, the chemical shifts were internally referenced to the solvent residual peak and in ^{31}P NMR, H_3PO_4 was used as external standard. For the simulation of NMR spectra, the experimental ^{1}H NMR spectrum was transferred to gNMR[3]. The full line shape iteration procedure of gNMR was applied to match the simulated to the experimental spectrum. Elemental analyses were performed with a Thermo Finnigan Flash EA 1112 Series. Spectro-electrochemical measurements were performed in $C_2H_4Cl_2$ solution with 0.26 M *n*-Bu_4NPF_6 as supporting electrolyte in an IR cell equipped with silver wire and platinum mesh. The compounds [Tp*W(CO)$_3$], [Tp*W(CO)I(Ph$_2$PC≡CH)],[4] [(C$_5$H$_5$)$_2$Fe]PF$_6$,[5] 2-ethynylpyridine,[6] [Ru(bpy)$_2$(PPh$_3$)Cl]PF$_6$,[7] [Ir(ppy)$_2$Cl]$_2$,[8] [Ru(dppp)$_2$Cl$_2$],[9] [Ru(bpy)$_2$(ppy)]PF$_6$[10] were synthesized according to literature procedures. All other reagents were used as purchased from commercial sources.

2.2 Synthetic procedures

PyC≡CCH$_3$

A yellow solution of 2-ethynylpyridine (2.66 g, 25.80 mmol) in 150 mL THF had been cooled to −78 °C for 15 min, before *n*-butyllithium (2.5 M solution in *n*-hexane, 14.4 mL, 36.11 mmol) was slowly added. The resulting red solution was stirred for 15 min at −78 °C to complete the reaction. After adding MeI (2.89 mL, 46.42 mmol) the solution turned orange and was stirred for 2 h at low temperatures. At room temperature the volatiles were removed *in vacuo* leaving an oily residue, which was purified on silica using a 3:2 mixture of *n*-hexane and ethyl acetate. Yield: 2.51 g, 83 %.

^{1}H NMR (300 MHz, $CDCl_3$, 300 K): δ [ppm] = 8.48 (d, $^{4}J_{H,H}$ = 0.8 Hz, $^{3}J_{H,H}$ = 4.9 Hz, 1H, Py-*H*), 7.55 (tdd, $^{4}J_{H,H}$ = 0.5 Hz, 1.9 Hz, $^{3}J_{H,H}$ = 7.8 Hz, 1H, Py-*H*), 7.30 (d, $^{4}J_{H,H}$ = 0.5 Hz, $^{3}J_{H,H}$ = 7.7 Hz, 1H, Py-*H*), 7.18 – 7.06 (m, 1H, Py-*H*), 2.03 (s, 3H, *C*H$_3$). **^{13}C NMR** (75 MHz, $CDCl_3$, 300 K): δ [ppm] = 149.8 (*C*-Py), 144.0 (*C$_{ipso}$*), 136.1, 126.6, 122.3 (3 *C*-Py), 86.6 (C*C*Py), 79.6 (C*C*CH$_3$), 4.3 (*C*H$_3$). **EA:** C_8H_7N (117.15 g/mol): C 82.49 (calcd. 82.02), H 5.66 (6.02), N 11.91 (11.96) %.

The analytical data is consistent with the literature.[11]

[Tp*W(CO)I(Ph$_2$PC≡CCH$_3$)] 1

A blue solution of [Tp*W(CO)I(Ph$_2$PC≡CH)] (800 mg, 0.90 mmol) in 45 mL THF had been cooled to −78 °C for 15 min, before *n*-butyllithium (2.5 M solution in *n*-hexane, 0.48 mL, 1.20 mmol) was slowly added. The resulting deep blue solution was stirred for 15 min at −78 °C to complete the reaction. After adding MeI (0.24 mL, 3.86 mmol) the solution was stirred for 4 h at low temperatures. Finally, all volatiles were removed at ambient temperature *in vacuo*, the green residue was purified on silica using a 1:1 mixture of CH_2Cl_2 and petroleum ether. Yield: 700 mg, 87 %.

^{1}H NMR (250 MHz, $CDCl_3$, 300 K): δ [ppm] = 7.31 – 7.21 (m, 5H, Ar-*H*), 7.13 (td, $^4J_{H,H}$ = 1.3 Hz, $^3J_{H,H}$ = 7.4 Hz, 1H, Ar-*H*), 6.89 (td, $^4J_{H,H}$ = 1.6 Hz, $^3J_{H,H}$ = 7.7 Hz, 2H, Ar-*H*), 6.54 (ddd, $^4J_{H,H}$ = 1.3 Hz, $^3J_{H,H}$ = 8.0 Hz, 9.0 Hz, 2H, Ar-*H*), 3.12 (s, 3H, CH_3), 2.75 (s, 3H, CH_3), 2.59 (s, 3H, CH_3), 2.34 (d, $^4J_{H,P}$ = 1.8 Hz, 3H, CH_3), 2.26 (s, 3H, CH_3), 2.24 (s, 3H, CH_3), 1.85 (s, 3H, CH_3), 1.80 (s, 3H, CH_3), 1.45 (s, 3H, CH_3), 1.36 (s, 3H, CH_3). **^{13}C NMR** (63 MHz, $CDCl_3$, 300 K): δ [ppm] = 233.1 (d, $^3J_{C,P}$ = 3.4 Hz, (W*C*O), 215.2 (d, $^3J_{C,P}$ = 3.3 Hz, C*C*CH_3), 206.3 (d, $^1J_{C,P}$ = 50.5 Hz, C*C*P), 153.2, 153.0, 148.8, 143.0, 141.9, 140.4, (9 *C*CH_3), 136.7 (d, $J_{C,P}$ = 11.5 Hz, C_{ipso}-Ar), 134.6 (d, $J_{C,P}$ = 1.5 Hz, C_{ipso}-Ar), 134.2, 134.0, 133.8, 133.7, 129.2, 128.4, 128.3, 128.1, 127.6, 127.4 (10 *C*-Ar), 113.4, 113.3, 113.2 (3 *C*CH_3), 24.0, 19.1, 18.9, 17.1, 11.4, 11.2, 10.8, 8.6, 8.4, 8.3 (10 C*C*H_3). **^{31}P{H} NMR** (101 MHz, $CDCl_3$, 300 K): δ [ppm] = 16.3 (s, C*C*P). **IR** (THF, cm^{-1}): $\tilde{\nu}$ = 2552 (w, BH), 1909 (s, CO); (CH_2Cl_2, cm^{-1}): $\tilde{\nu}$ = 2548 (w, BH), 1893 (s, CO). **EA** $C_{34}H_{41}BIN_6OPW$ (902.27 g/mol): C 45.47 (calcd. 45.26), H 4.62 (4.58), N 9.24 (9.31) %.

[Tp*W(CO)Br(PyC≡CCH$_3$)] 2

A red solution of [Tp*W(CO)$_3$] (6.0 g, 9.88 mmol) and 2-(prop-1-yne-1-yl)pyridine (1.16 g, 9.88 mmol) in 110 mL CH_2Cl_2 was cooled to 0 °C and treated with solid $[(C_5H_5)_2Fe]PF_6$ (3.27 g, 9.88 mmol) in small portions within 30 min. After stirring at room temperature for 2 h *in situ* IR-measurements confirmed the complete formation of $[Tp^*W(CO)_2(PyCCCH_3)]^+$ [$\tilde{\nu}$ = 2565 (w, BH), 2057, 1920 (s, CO)]. All volatiles were removed *in vacuo*. The brown residue was dissolved in 110 mL THF and solid NBu_4Br (3.84 g, 11.91 mmol) was added. After 2 h at room temperature the completion of the CO substitution was confirmed by *in situ* IR spectroscopy. All volatiles were removed *in vacuo* and the crude product was washed several times with methanol. After drying *in vacuo* the residue was purified on silica using a 10:1 mixture of CH_2Cl_2 and CH_3CN. Yield: 2.57 g, 35 %.

^{1}H NMR (300 MHz, $CDCl_3$, 298 K): δ [ppm] = 8.66 (ddd, $^4J_{H,H}$ = 0.9, 1.9 Hz, $^3J_{H,H}$ = 4.8 Hz, 1H, Ar-*H*), 7.30 (td, $^4J_{H,H}$ = 1.9 Hz, $^3J_{H,H}$ = 7.7 Hz, 1H, Ar-*H*), 7.07 (ddd, $^4J_{H,H}$ = 1.3 Hz, $^3J_{H,H}$ = 4.8 Hz, 7.6 Hz, 1H, Ar-*H*), 5.76 (dt, $^4J_{H,H}$ = 1.1 Hz, $^3J_{H,H}$ = 7.8 Hz, 1H, Ar-H), 3.72 (s, 3H, CH_3), 2.82 (s, 3H, CH_3), 2.48 (s, 3H, CH_3), 2.45 (s, 3H, CH_3), 2.28 (s, 3H, CH_3), 1.84 (s, 3H, CH_3), 1.74 (s, 3H, CH_3), 1.70 (s, 3H, CH_3), 1.65 (s, 3H, CH_3), 1.38 (s, 3H, CH_3). **^{13}C NMR** (126 MHz, $CDCl_3$, 298 K): δ [ppm] = 232.4 (W*C*O), 208.4 (C*C*CH_3), 206.2 (C*C*Py), 157.1 (C_{ipso}-Ar), 152.7, 152.4, 149.4 (3 *C*CH_3), 148.3 (*C*-Ar), 143.0, 142.0, 140.6 (3 *C*CH_3), 136.2 (*C*-Ar), 125.3, 122.4 (2 *C*-Ar), 113.9, 113.2, 112.5 (3 *C*CH_3), 22.4, 15.1, 14.5, 14.4, 11.1, 11.1, 10.9, 8.4, 8.2, 8.1 (10 *C*H_3). **IR** (THF, cm^{-1}) = 2551 (w, BH), 1906 (s, CO); (ATR, cm^{-1}) = 2553 (w, BH), 1893 (s, CO). **EA** $C_{27}H_{35}BBrN_7OW$ (748.18 g/mol): C 43.89 (calcd. 43.34), H:4.63 (4.72), N 12.65 (13.11) %.

[Tp*W(CO)I(Ph$_2$PC≡CCH$_2$)]$_2$ [3]$_2$

A green solution of **1** (100 mg, 0.11 mmol) in 15 mL THF had been cooled to −78 °C for 15 min, before *n*-butyllithium (2.5 M solution in *n*-hexane, 0.06 mL, 0.15 mmol) was slowly added. The resulting red solution was stirred for 5 min at −78 °C. After slowly adding a solution of $[RuCl_2(dppp)_2]PF_6$ (128 mg, 0.11 mmol) in 3 mL THF, the reaction mixture was stirred at low temperatures for 3 h. All volatiles were removed *in vacuo* and 15 mL CH_2Cl_2 was added. After filtration, the solution was concentrated and crystallized by slow diffusion of *n*-pentane into the concentrated solution. Yield: 15 mg, 13 %.

^{1}H NMR (500 MHz, $CDCl_3$, 298 K): δ [ppm] = 7.41 – 7.33 (m, 4H, Ar-*H*), 7.20 – 7.16 (m, 6H, Ar-*H*), 7.13 (td, $^4J_{H,H}$ = 1.3 Hz, $^3J_{H,H}$ = 7.4 Hz, 2H, Ar-*H*), 6.91 (td, $^4J_{H,H}$ = 1.5 Hz, $^3J_{H,H}$ = 7.6 Hz, 4H, Ar-*H*), 6.60 (t, $^3J_{H,H}$ = 7.8 Hz, 4H, Ar-*H*), 4.16 – 3.74 (m, 4H, CH_2), 2.76 (s, 6H, CH_3), 2.60 (s, 6H, CH_3), 2.46 (d,

$^{4}J_{H,H}$ = 1.6 Hz, 6H, CH_3), 2.28 (s, 6H, CH_3), 2.23 (s, 6H, CH_3), 1.85 (s, 6H, CH_3), 1.79 (s, 6H, CH_3), 1.46 (s, 6H, CH_3), 1.39 (s, 6H, CH_3). **^{13}C NMR** (126 MHz, $CDCl_3$, 298 K): δ [ppm] = 153.1, 153.0, 149.1, 142.9, 141.7, 140.4 (6 *C*CH_3), 134.4, 134.2, 134.0, 129.7, 128.9, 128.9, 128.0, 127.5, 127.4 (9 *C*-Ar), 113.3 (*C*CH_3), 32.7 (*C*H_2), 19.3, 17.3, 14.7, 11.4, 11.3, 10.9, 8.7, 8.5, 8.4 (9 CH_3); the quaternary carbon atoms (W*C*O, C*C*P, *C*CP, and C_{ipso}) could not be detected due to low solubility. **^{31}P{H} NMR** (122 MHz, $CDCl_3$, 298 K): δ [ppm] = 15.3 (s, CC*P*). **IR** (CH_2Cl_2, cm^{-1}): $\tilde{\nu}$ = 2558 (w, BH), 1920 (s, CO). **EA** $C_{68}H_{80}B_2I_2N_{12}O_2P_2W_2$ (1802.53 g·mol^{-1}): C 45.31 (calcd. 45.31), H 4.48 (4.47), N 9.39(9.32).

[Tp*W(CO)I(Ph$_2$PC≡CCH$_2$)Au]$_2$ 5

A green solution of **1** (100 mg, 0.11 mmol) in 8 mL THF had been cooled to −78 °C for 15 min, before *n*-butyllithium (2.5 M solution in *n*-hexane, 0.06 mL, 0.15 mmol) is slowly added. The resulting red solution was stirred for 10 min at −78 °C. In the dark a solution of $AuSMe_2Cl$ (33 mg, 0.11 mmol) in 5 mL THF was slowly added, the reaction mixture was stirred at low temperatures for 3 h. All volatiles were removed *in vacuo* and 15 mL CH_2Cl_2 was added. After filtration, the solution was concentrated and crystallized by slow diffusion of *n*-pentane into the concentrated solution. Yield: 48 mg, 38 % (with both isomers being present). The isomers were separated by fractionated crystallisation, showing that the *unlike*-**5** is more soluble in CH_2Cl_2 compared to *like*-**5.**

While we were able to isolate the *unlike*-isomer in pure form allowing full characterization by NMR and IR spectroscopy as well as cyclic voltammetry, the *like*-isomer was solely investigated in a 2:3 mixture with the *unlike*-isomer by ^{31}P NMR and IR spectroscopy. To proof the different connectivity, XRD analysis was performed for both isomers.

unlike-**5**

^{1}H NMR (500 MHz, CD_2Cl_2, 298 K): δ [ppm] = 7.54 (ddd, $^{4}J_{H,H}$ = 1.4 Hz, $^{3}J_{H,H}$ = 8.3 Hz, 13.0 Hz, 4H, Ar-*H*), 7.33 – 7.28 (m, 4H, Ar-*H*), 7.21 (td, $^{4}J_{H,H}$ = 2.2 Hz, $^{3}J_{H,H}$ = 7.7 Hz, 4H, Ar-*H*), 7.10 – 7.04 (m, 8H, Ar-*H*), 4.50 (ddd, $^{4}J_{H,P}$ = 2.0 Hz, $^{2}J_{H,H}$ = 6.7 Hz, $^{3}J_{H,P}$ = 11.5 Hz, 2H), 3.84 (ddd, $^{4}J_{H,P}$ = 2.0 Hz, $^{1}J_{H,H}$ = 6.7 Hz, $^{3}J_{H,P}$ = 8.5 Hz, 2H), 2.73 (s, 6H, CH_3), 2.60 (s, 6H, CH_3), 2.51 (s, 6H, CH_3), 2.43 (s, 6H, CH_3), 2.29 (s, 6H, CH_3), 1.83 (s, 12H, CH_3), 1.43 (s, 6H, CH_3), 1.18 (s, 6H, CH_3). **^{31}P{H} NMR** (202 MHz, CD_2Cl_2, 298 K): δ [ppm] = 45.9 (s, CC*P*). **IR** (THF, cm^{-1}): $\tilde{\nu}$ = 2556 (w, BH), 1900 (s, CO); (CH_2Cl_2, cm^{-1}): $\tilde{\nu}$ = 2554 (w, BH), 1894 (s, CO). **EA** $C_{68}H_{80}Au_2B_2I_2N_{12}O_2P_2W_2$ (2196.46 g/mol): C 37.81 (calcd. 38.12), H 3.91 (3.91), N 7.36 (7.41). Recording of a meaningful ^{13}C NMR spectrum failed due to the low solubility of the compound.

like-**5**

^{31}P{H} NMR (101 MHz, THF-d^8, 298 K): δ [ppm] = 51.3 (s, CC*P*). **IR** (THF, cm^{-1}): $\tilde{\nu}$ = 2556 (w, BH), 1900 (s, CO); (CH_2Cl_2, cm^{-1}): $\tilde{\nu}$ = 2554 (w, BH), 1894 (s, CO).

[Tp*W(CO)(Br)(PyC≡CCH$_2$)-Ru(bpy)$_2$][PF$_6$] 6-PF$_6$

To a green suspension of **2** (300 mg, 0.40 mmol) and $[Ru(bpy)_2(PPh_3)Cl][PF_6]$ (428 mg, 0.50 mmol) in 30 mL THF a KO*t*Bu solution (0.1 M in THF, 0.38 mmol) was added dropwise. The red reaction mixture was heated under reflux for 4 h. All volatiles were removed *in vacuo* the residue was purified on silica

using a 10:1 mixture of CH_2Cl_2 and CH_3CN. For further purification, the product was recrystallized from CH_2Cl_2 and diethyl ether. Yield: 342 g, 66 %.

^{1}H NMR (300 MHz, CD_2Cl_2, 298 K): δ [ppm] = 9.06 (d, $^3J_{H,H}$ = 5.6 Hz, 1H, Ar-*H*), 8.55 (d, $^3J_{H,H}$ = 8.1 Hz, 1H, Ar-*H*), 8.48 (d, $^3J_{H,H}$ = 8.1 Hz, 1H, Ar-*H*), 8.12 (dd, $^3J_{H,H}$ = 8.1 Hz, 12.7 Hz, 2H, Ar-*H*), 8.06 – 7.96 (m, 2H, Ar-*H*), 7.86 (td, $^4J_{H,H}$ = 1.5 Hz, $^3J_{H,H}$ = 7.8 Hz, 1H, Ar-*H*), 7.78 – 7.70 (m, 2H, Ar-*H*), 7.70 – 7.61 (m, 1H, Ar-*H*), 7.49 – 7.40 (m, 4H, Ar-*H*), 7.38 (d, $^3J_{H,H}$ = 5.7 Hz, 1H, Ar-*H*), 7.28 – 7.17 (m, 1H, Ar-*H*), 7.06 (t, $^3J_{H,H}$ = 6.6 Hz, 1H, Ar-*H*), 7.00 (t, $^3J_{H,H}$ = 6.6 Hz, 1H, Ar-*H*), 6.76 (d, $^3J_{H,H}$ = 7.8 Hz, 1H, Ar-*H*), 6.70 – 6.59 (m, 1H, *Ar*-H), 4.40 (d, $^1J_{H,H}$ = 18.4 Hz, 1H, C*H*$_2$), 2.59 (s, 3H, C*H*$_3$), 2.53 (s, 3H, C*H*$_3$), 2.41 (s, 3H, C*H*$_3$), 2.29 (s, 3H, C*H*$_3$), 2.18 (s, 3H, C*H*$_3$), 2.05 – 1.95 (m, 3H, C*H*$_3$), 2.05 – 1.95 (m, 1H, C*H*$_2$), 1.98 (s, 3H, C*H*$_3$), 1.82 (s, 3H, C*H*$_3$), 1.73 (s, 3H, C*H*$_3$), 1.56 (s, 3H, C*H*$_3$). **^{13}C NMR** (75 MHz, CD_2Cl_2, 298 K): δ [ppm] = 230.5 (W*C*O), 224.7 (C*C*CH$_2$), 204.7 (C*C*Py), 159.9, 158.9, 158.1, 156.4, 156.1 (5x C_{ipso}-Ar), 152.8 (*C*CH$_3$), 152.5 (*C*-Ar), 152.0 (*C*CH$_3$), 151.8, 151.6, 150.7, 149.5 (4x *C*-Ar), 149.3 , 143.8, 142.6, 142.0 (4x*C*CH$_3$), 137.3 (*C*-Ar) , 136.1 (2x *C*-Ar), 134.3, 133.6, 128.5, 127.4, 126.9, 126.4, 125.7, 124.9, 124.4, 123.3, 123.2, 122.9 (12x *C*-Ar), 114.1, 113.8, 113.1 (3xC*C*H$_3$), 26.9 (*C*H$_2$), 15.7, 15.4, 14.9 (3xC*C*H$_3$), 11.4 (2xC*C*H$_3$), 11.3, 8.6, 8.5, 8.4 (4xC*C*H$_3$). **^{31}P{H} NMR** (122 MHz, CD_2Cl_2, 298 K): δ [ppm] = −144.46 (hept, $^1J_{P,F}$ = 711.0 Hz, *P*F$_6$). **IR** (THF, cm^{-1}): $\tilde{\nu}$ = 2553 (w, BH), 1893 (s, CO); (CH_2Cl_2, cm^{-1}): $\tilde{\nu}$ = 2559 (w, BH), 1889 (s, CO); (ATR, cm^{-1}): $\tilde{\nu}$ = 2549 (w, BH), 1877 (s, CO). **EA** $C_{47}H_{50}BBrF_6N_{11}OPRuW \cdot 0.5\ CH_2Cl_2$ (1348.05 g/mol): C 42.57 (calcd. 42.32), H 3.75 (3.81), N 11.40 (11.43) %.

[Tp*W(CO)(Br)(PyC≡CCH$_2$)-Ir(ppy)$_2$] 7

To a suspension of **2** (400 mg, 0.53 mmol) and $(Ir(ppy)_2Cl)_2$ (558 mg, 0.97 mmol) in 40 mL THF a KO*t*Bu solution (0.1 M in THF, 0.64 mmol) was added dropwise. The red reaction mixture was headed under reflux for 5 h. After filtration over celite, all volatiles were removed *in vacuo* and the residue was purified by recrystallisation from CH_2Cl_2 and diethyl ether. Yield: 374 g, 57 %.

^{1}H NMR (300 MHz, CD_2Cl_2, 298 K): δ [ppm] = 9.02 (d, $^3J_{H,H}$ = 5.9 Hz, 1H, Ar-*H*), 8.09 – 8.01 (m, 1H, Ar-*H*), 7.98 – 7.92 (m, 1H, Ar-*H*), 7.75 (d, $^3J_{H,H}$ = 6.3 Hz, 3H, Ar-*H*), 7.70 – 7.60 (m, 1H, Ar-*H*), 7.52 (dd, $^4J_{H,H}$ = 1.5 Hz, $^3J_{H,H}$ = 7.7 Hz, 2H, Ar-*H*), 7.39 (td, $^4J_{H,H}$ = 1.7 Hz, $^3J_{H,H}$ = 7.6 Hz, 1H, Ar-*H*), 6.97 – 6.87 (m, 2H, Ar-*H*), 6.83 (td, $^4J_{H,H}$ = 1.3 Hz, $^3J_{H,H}$ = 7.2 Hz, 1H, Ar-*H*), 6.75 (td, $^4J_{H,H}$ = 1.3 Hz, $^3J_{H,H}$ = 7.4 Hz, 1H, Ar-*H*), 6.68 – 6.58 (m, 4H, Ar-*H*), 6.56 (dd, $^4J_{H,H}$ = 1.4 Hz, $^3J_{H,H}$ = 7.3 Hz, 1H, Ar-*H*), 6.08 (dd, $^4J_{H,H}$ = 1.2 Hz, $^3J_{H,H}$ = 7.7 Hz, 1H, Ar-*H*), 4.32 (d, $^2J_{H,H}$ = 18.7 Hz, 1H, C*H*$_2$), 2.86 (d, $^2J_{H,H}$ = 18.9 Hz, 1H, C*H*$_2$), 2.69 (s, 3H, C*H*$_3$), 2.49 (s, 3H, C*H*$_3$), 2.39 (s, 3H, C*H*$_3$), 2.25 (s, 3H, C*H*$_3$), 2.07 (s, 3H, C*H*$_3$), 1.89 (s, 3H, C*H*$_3$), 1.79 (s, 3H, C*H*$_3$), 1.69 (s, 3H, C*H*$_3$), 1.53 (s, 3H, C*H*$_3$). **^{13}C NMR** (75 MHz, CD_2Cl_2, 298 K): δ [ppm] = 229.9 (W*C*O), 225.8 (C*C*Py), 202.1 (C*C*CH$_2$), 178.1, 171.5, 166.4, 157.3 (4 C_{ipso}-Ar), 153.4 (*C*-Ar), 153.0, 151.6 (2 *C*CH$_3$), 151.1 (C_{ipso}-Ar), 150.30, 149.5 (2 *C*-Ar), 148.9 (*C*CH$_3$), 144.5, 143.3 (2 C_{ipso}-Ar), 142.3, 141.4, 140.8 (3 *C*CH$_3$), 137.5, 136.0, 134.5, 132.5 (4 *C*-Ar), 130.3 (2 *C*-Ar), 128.5, 125.8, 125.0, 123.7, 123.3, 122.3, 121.5, 120.7, 119.5, 119.3, 118.8 (11 *C*-Ar), 113.3, 113.2, 112.2 (3 *C*CH$_3$), 25.8 (*C*H$_2$), 15.5, 15.1, 14.6 (3 C*C*H$_3$), 11.3 (3 C*C*H$_3$), 8.6, 8.4, 8.4 (3 C*C*H$_3$). **IR** (THF, cm^{-1}): $\tilde{\nu}$ = 2550 (w, BH), 1891 (s, CO); (CH_2Cl_2, cm^{-1}): $\tilde{\nu}$ = 2555 (w, BH), 1887 (s, CO); (ATR, cm^{-1}): $\tilde{\nu}$ = 2553 (w, BH), 1885 (s, CO). **EA** $C_{49}H_{50}BBrIrN_9OW \cdot CH_2Cl_2$ (1332.70 g/mol): C 45.01 (calcd. 45.06), H 3.78 (3.93), N 9.55 (9.46) %.

2.3 NMR spectra

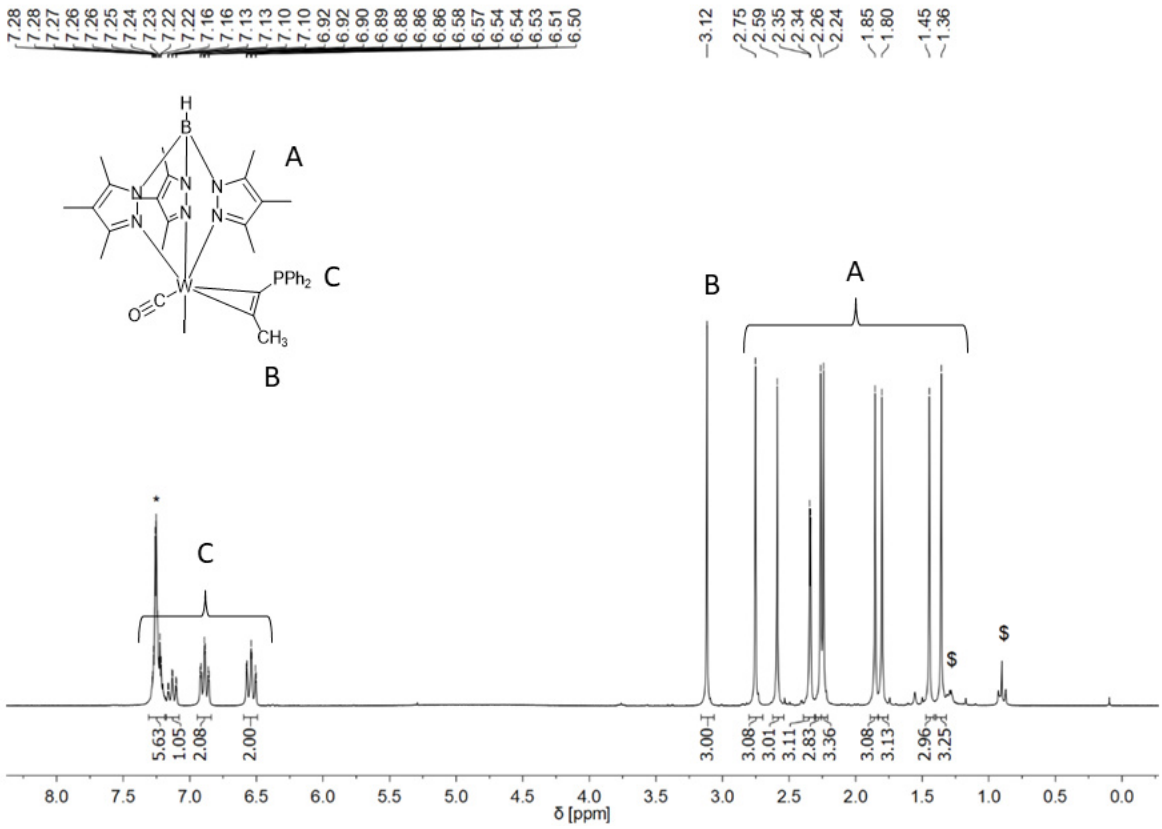

Figure S5. ^{1}H NMR of **1** in $CDCl_3$ (*); $ *n*-pentane.

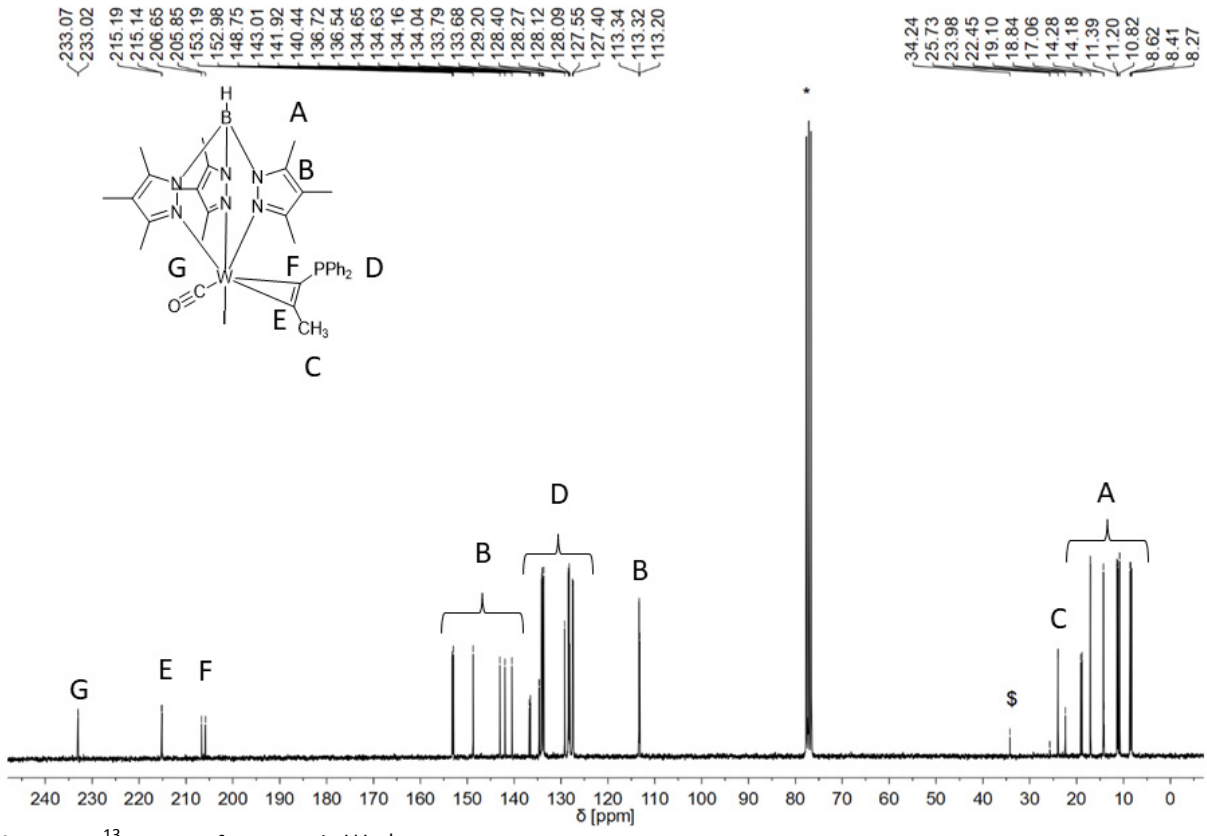

Figure S6. ^{13}C NMR of **1** in $CDCl_3$ (*); $ *n*-pentane.

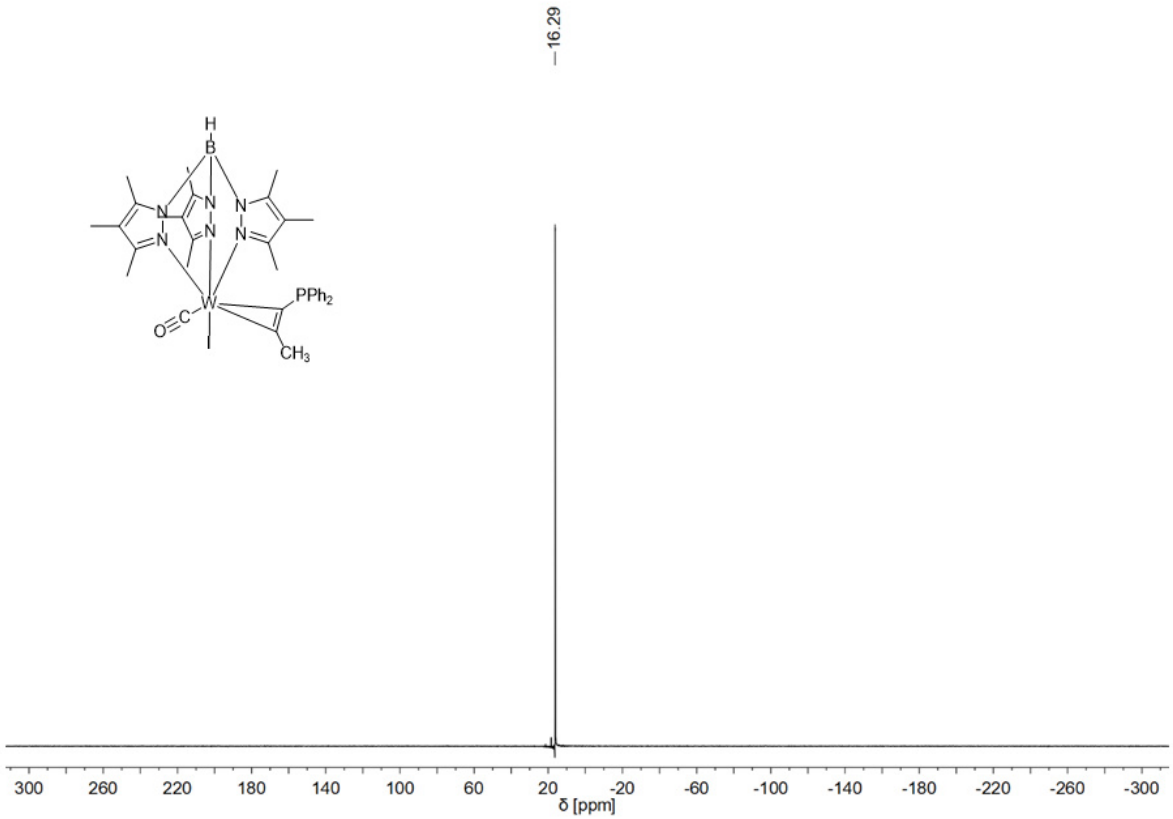

Figure S7. ^{31}P NMR of **1** in $CDCl_3$.

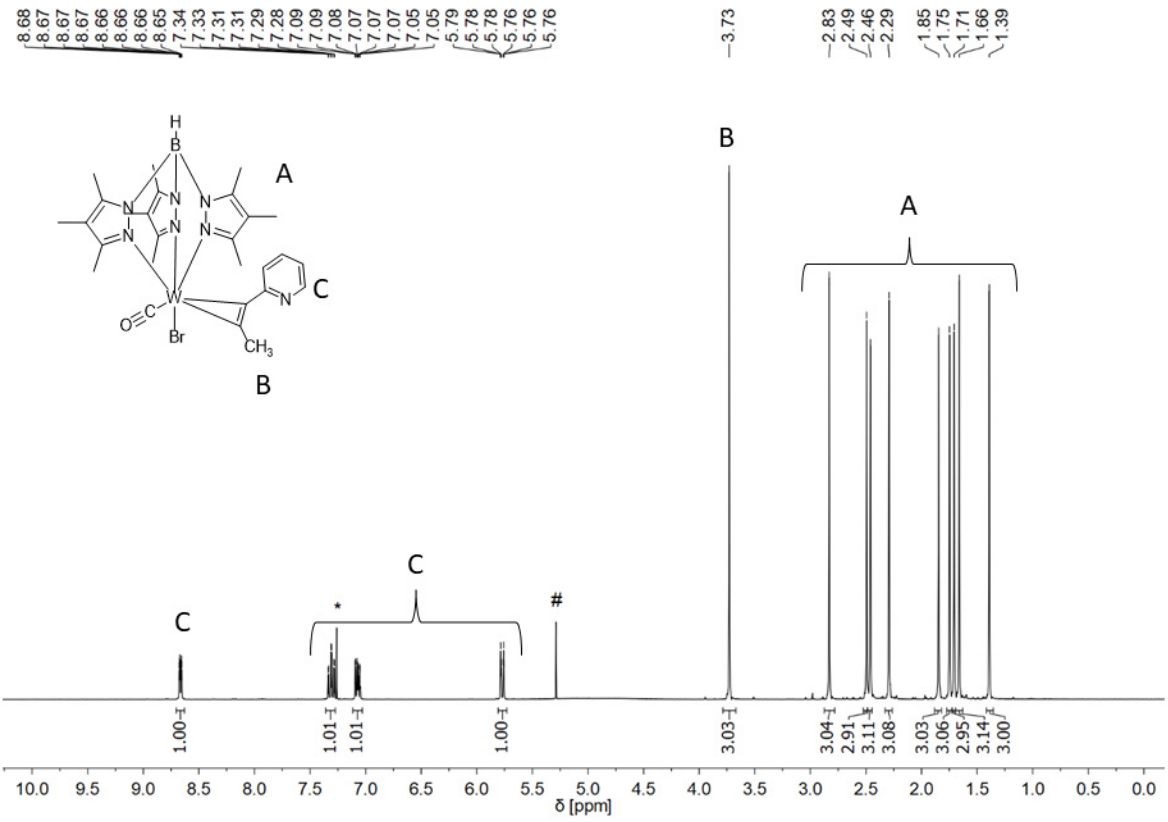

Figure S8. ^{1}H NMR of **2** in $CDCl_3$ (*); # CH_2Cl_2.

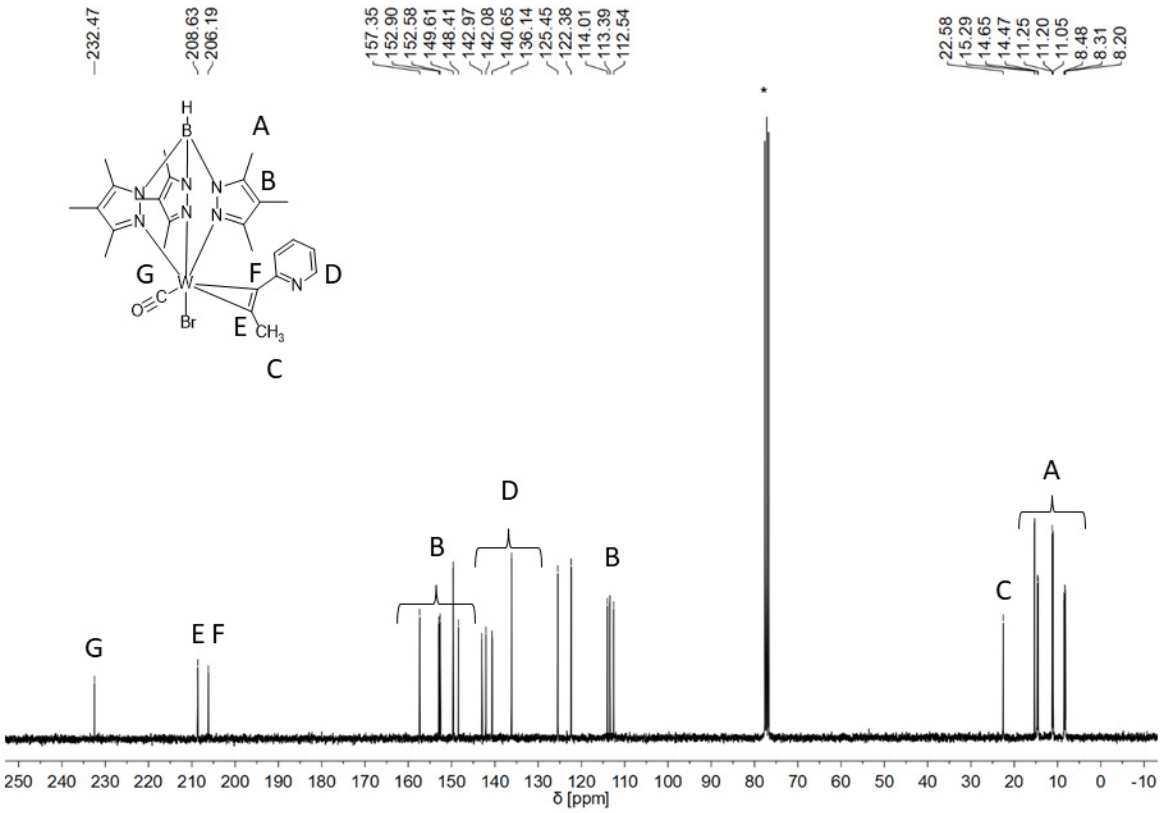

Figure S9. ^{13}C NMR of **2** in $CDCl_3$ (*).

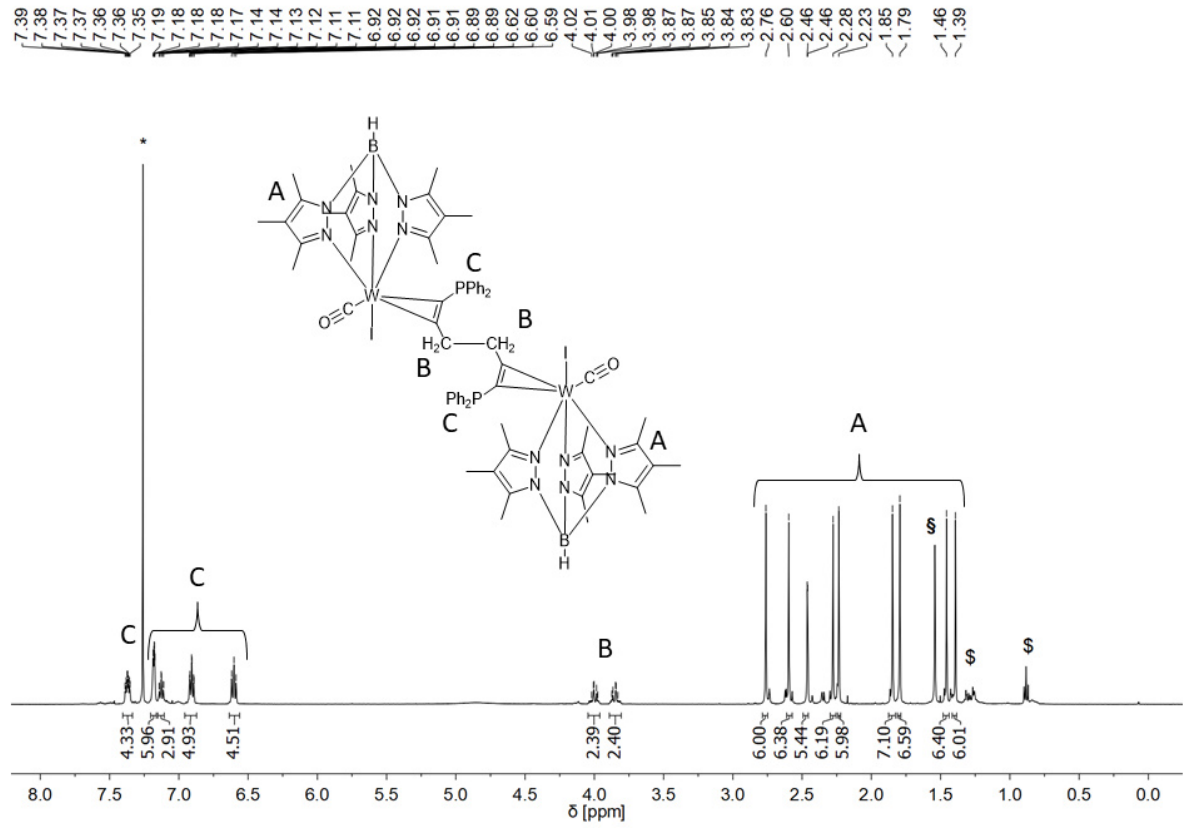

Figure S10. ^{1}H NMR of [**3**]$_2$ in $CDCl_3$ (*); § water; $ *n*-pentane.

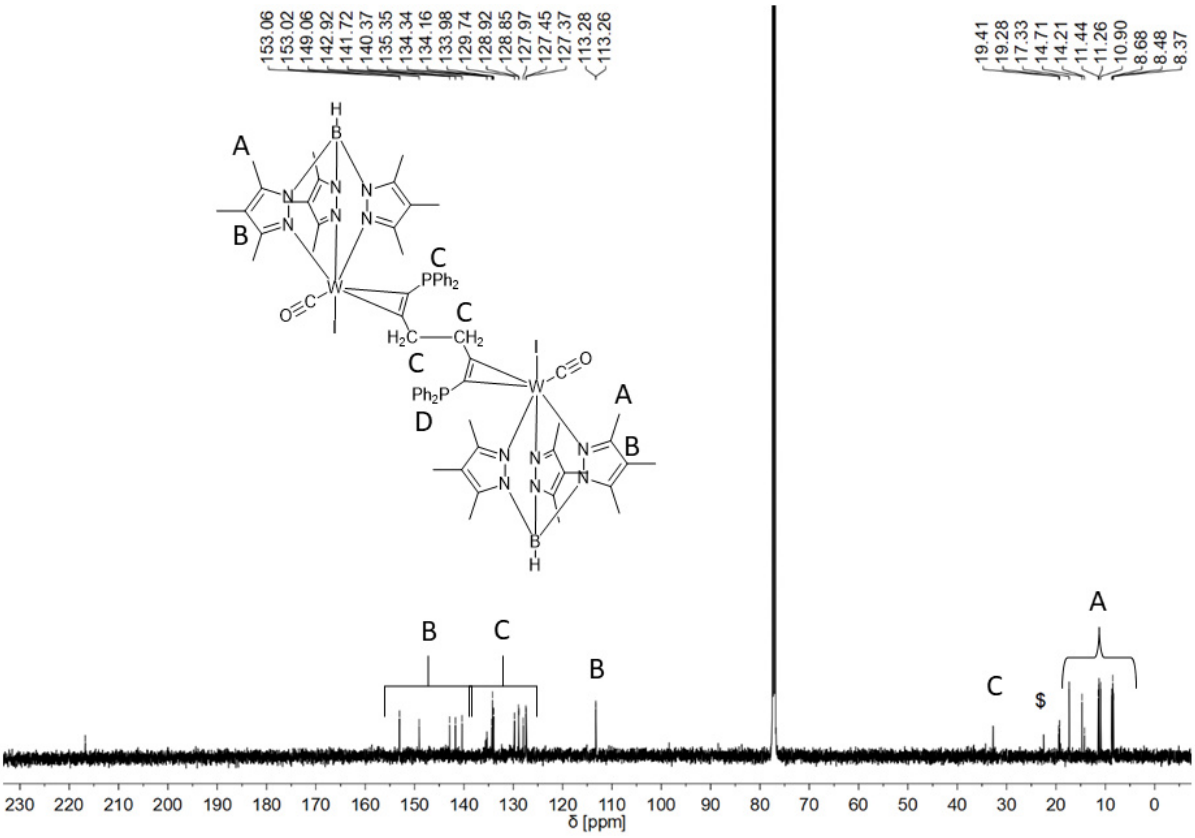

Figure S11. ^{13}C NMR of [**3**]$_2$ in $CDCl_3$ (*); $ *n*-pentane.

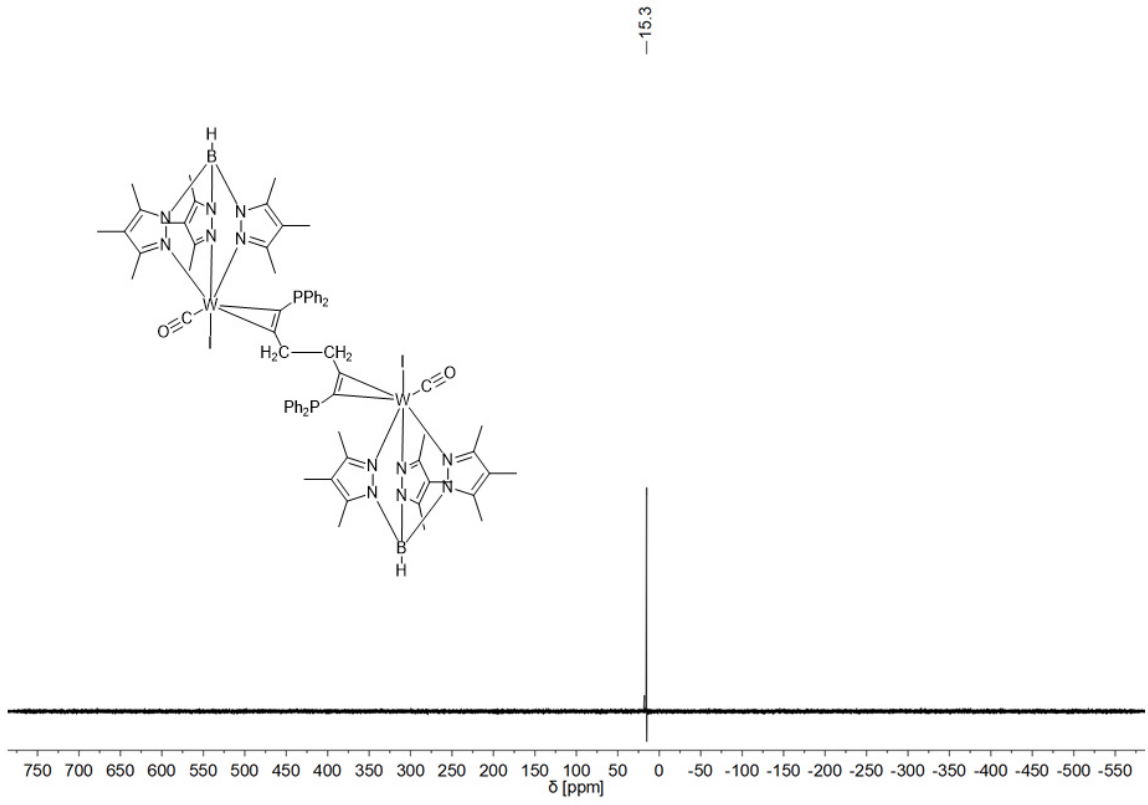

Figure S12. ^{31}P NMR of [**3**]$_2$ in $CDCl_3$.

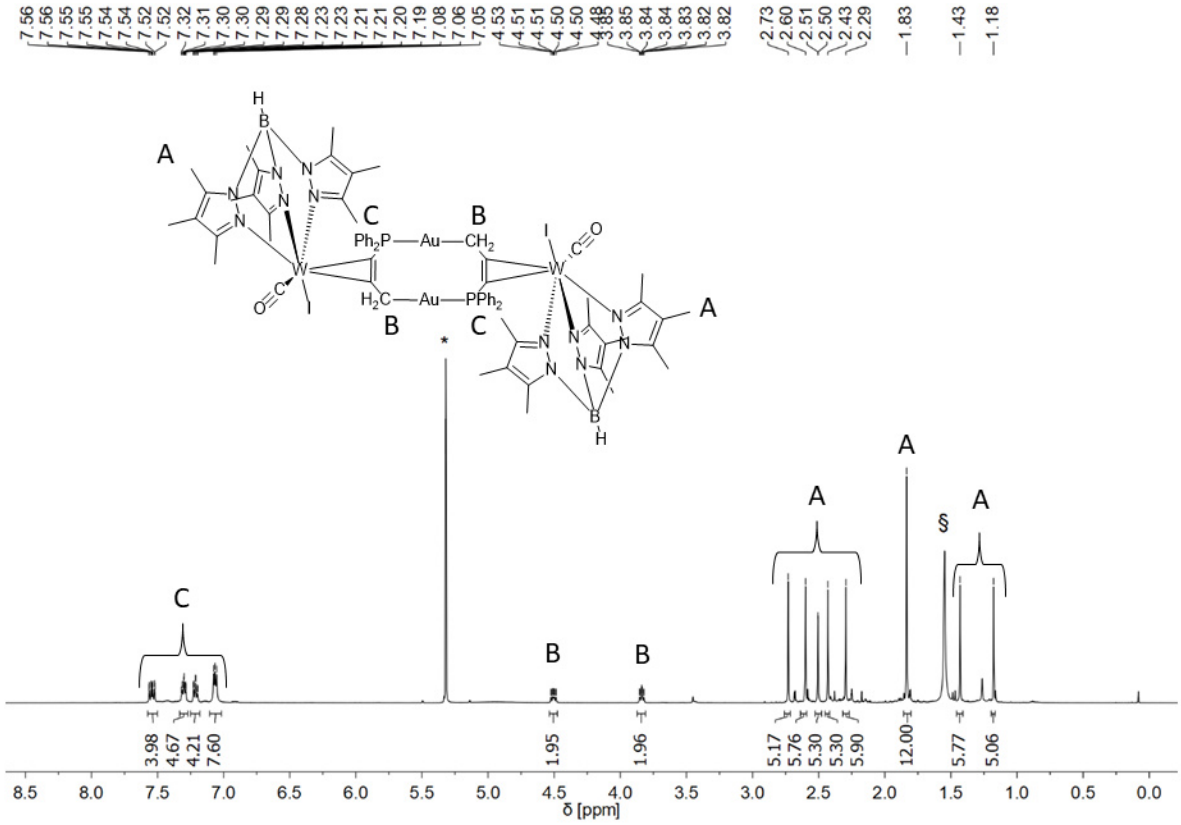

Figure S13. ^{1}H NMR of *unlike*-**5** in CD_2Cl_2 (*); § water.

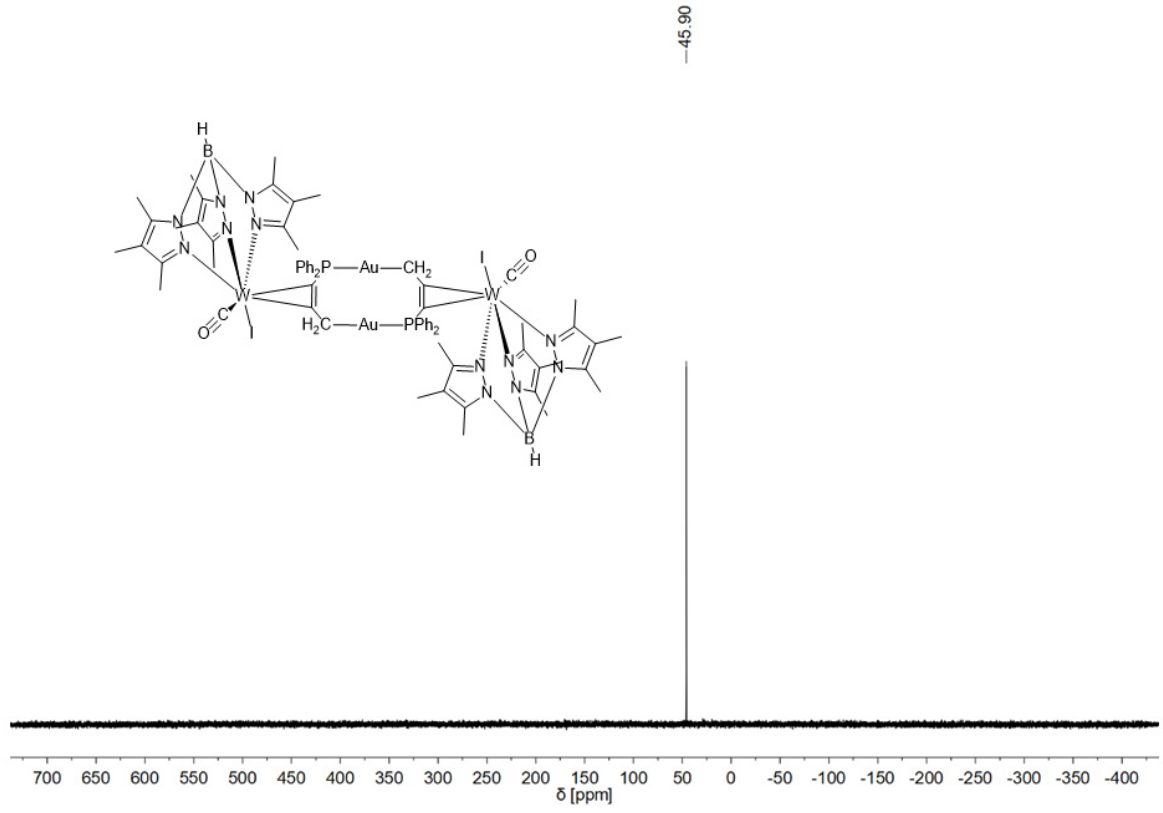

Figure S14. ^{31}P NMR of *unlike*-**5** in CD_2Cl_2.

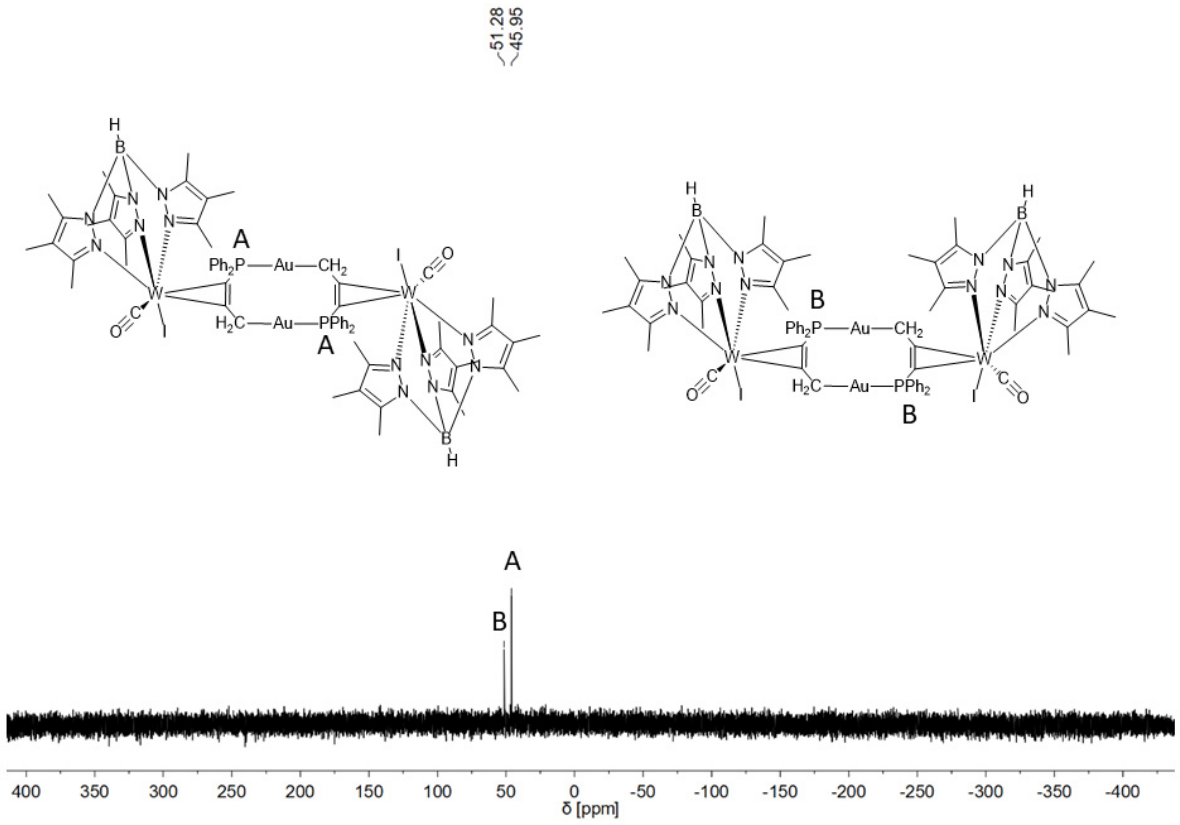

Figure S15. ^{31}P NMR of *like*-**5** and *unlike*-**5** in CD_2Cl_2.

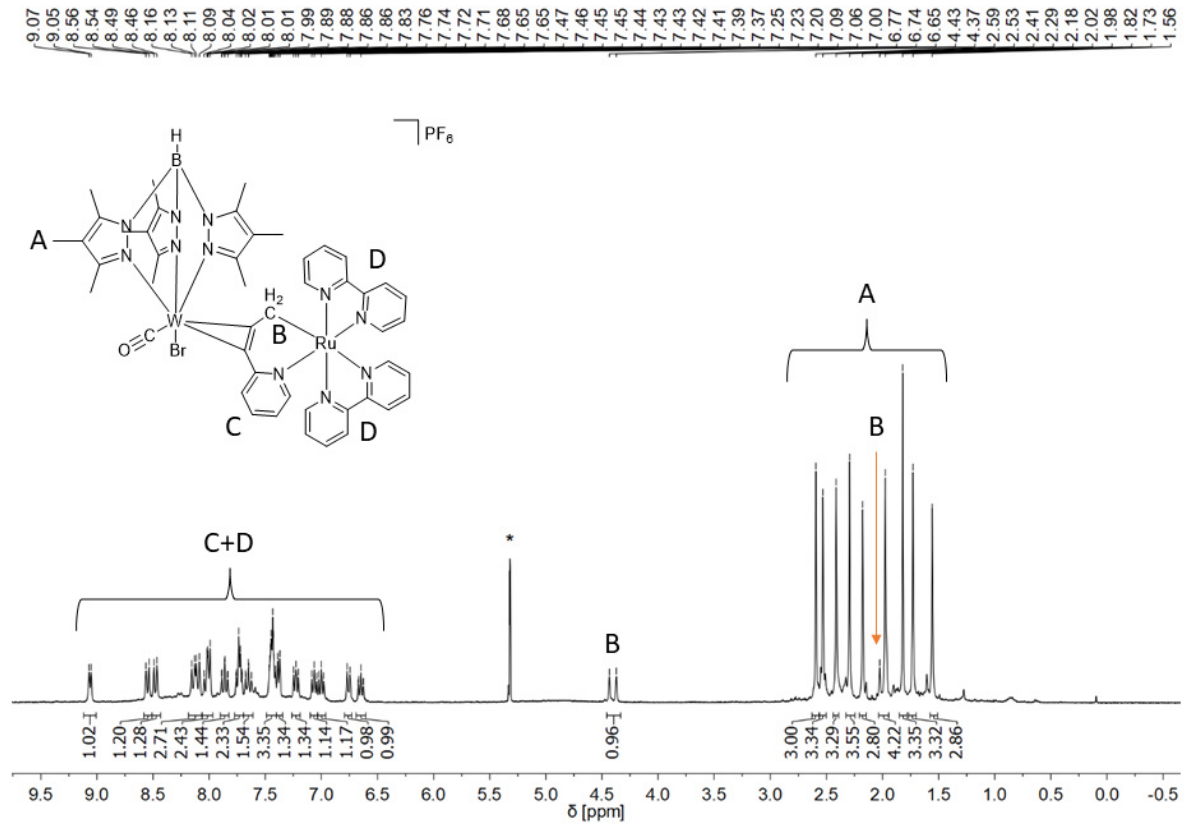

Figure S16. ^{1}H NMR of **6**-PF_6 in CD_2Cl_2 (*).

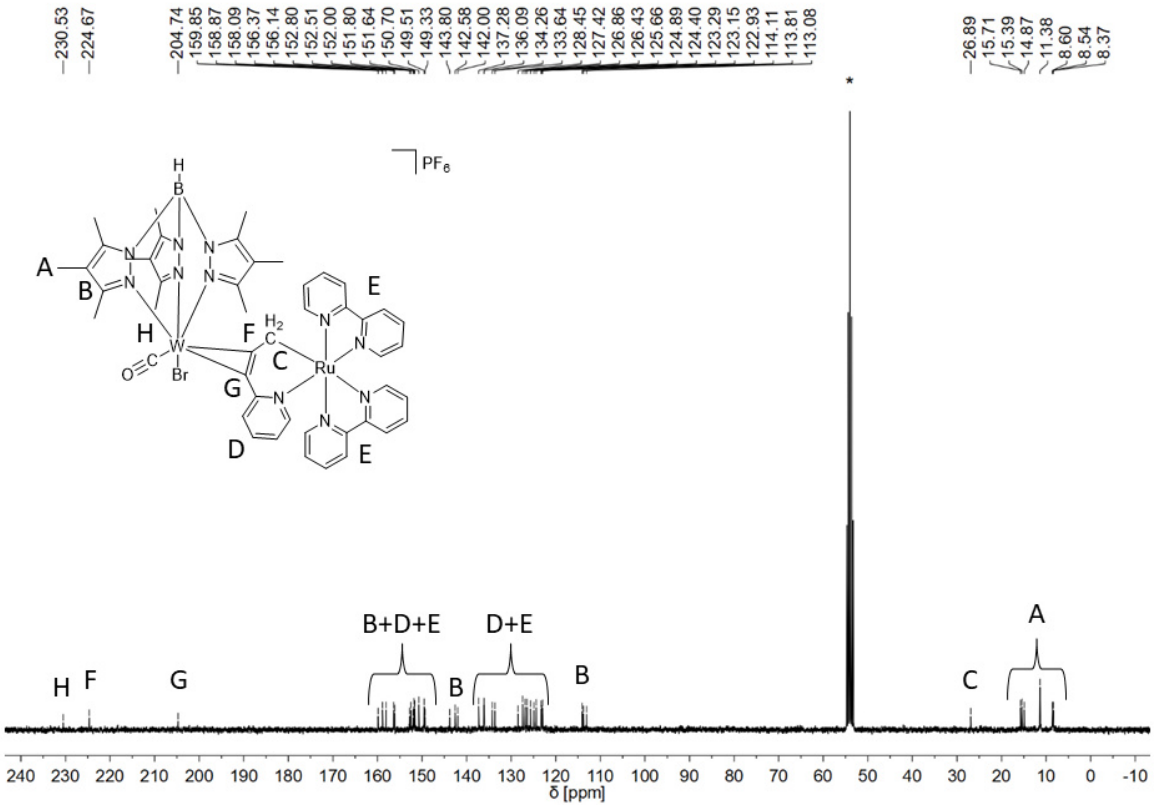

Figure S17. ^{13}C NMR of **6**-PF_6 in CD_2Cl_2 (*).

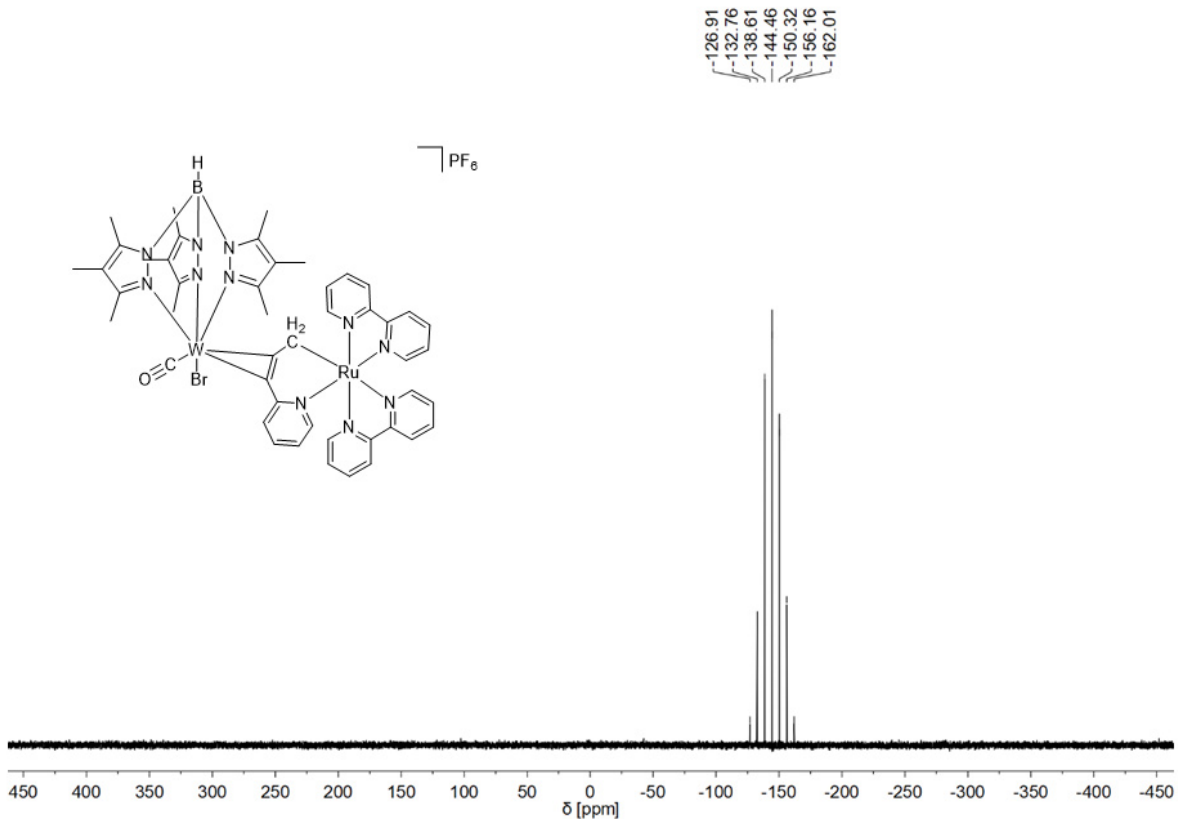

Figure S18. ^{31}P NMR of **6**-PF_6 in CD_2Cl_2 (*).

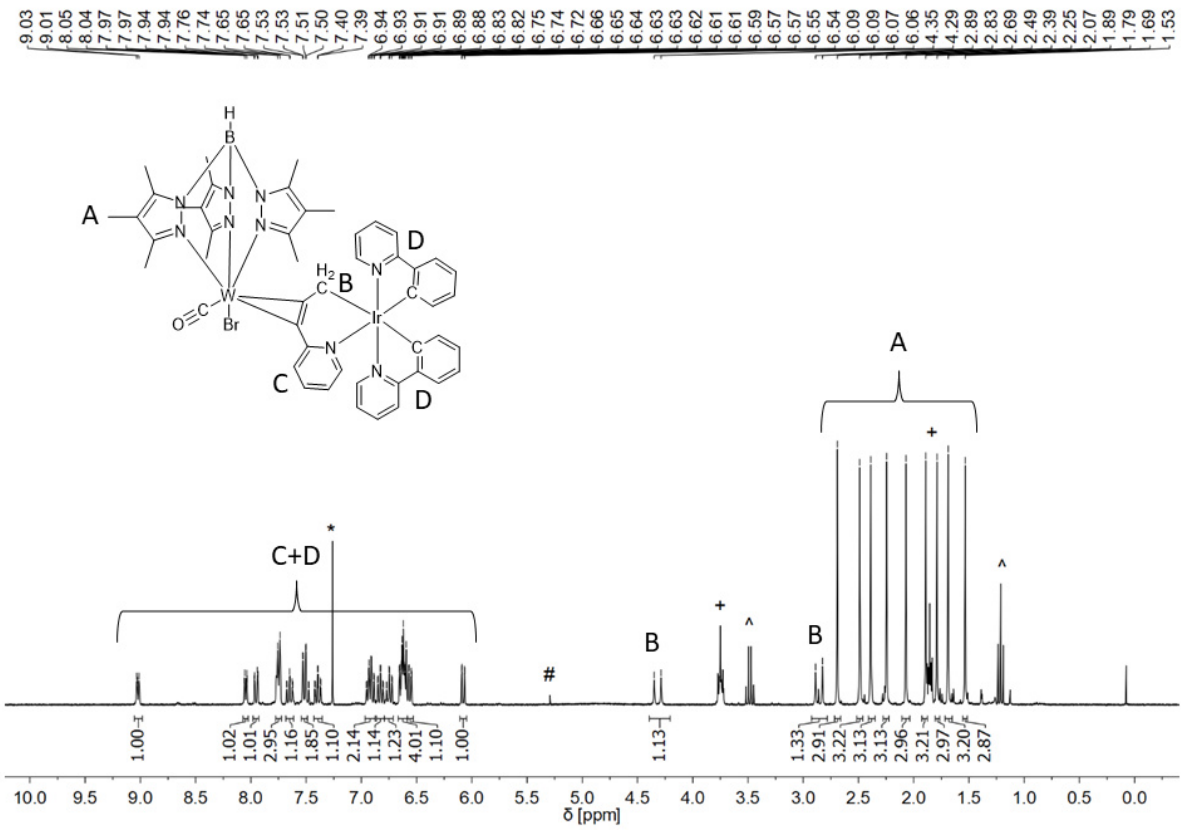

Figure S19. ^{1}H NMR of **7** in $CDCl_3$ (*); # CH_2Cl_2; + THF; ^ $C_4H_{10}O$.

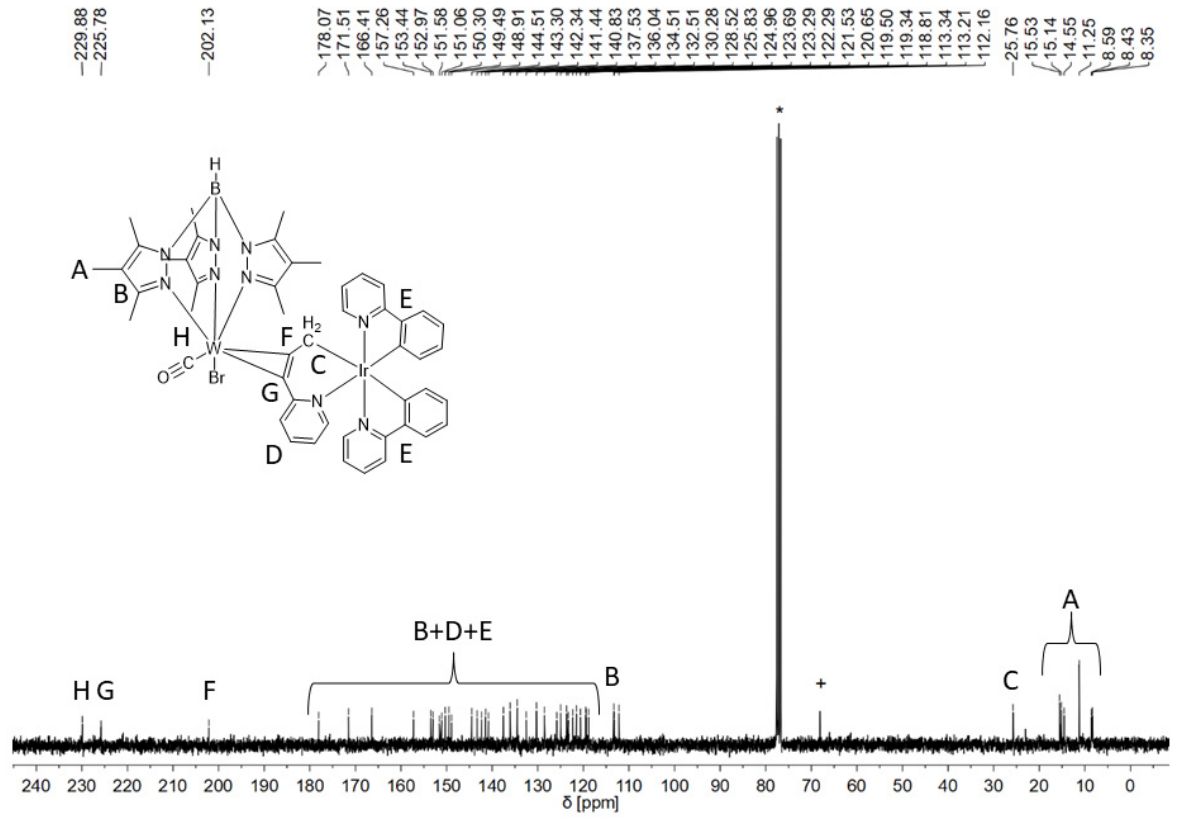

Figure S20. ^{13}C NMR of **7** in $CDCl_3$ (*); + THF.

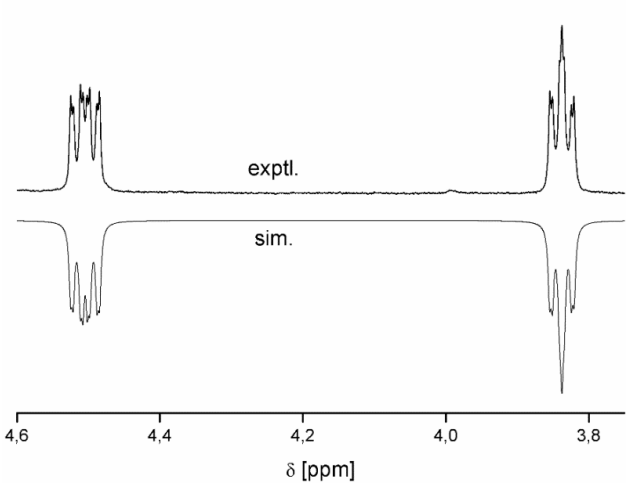

Figure S21. ^{1}H NMR spectrum of *unlike*-**5**, the simulated NMR spectrum (bottom) and experimental NMR data (top) are in good agreement.

Table S3. ^{1}H and ^{31}P NMR data of *unlike*-**5**, simulated values are given in brackets.

	δ [ppm]	J [Hz]	J [Hz]
H_A	4.50		
H_B	3.84	$J_{A,B}$ = 6.7 (6.8)	
P_C	45.9	$J_{A,C}$ = 2.0 (1.9)	$J_{B,C}$ = 8.5 (8.4)
P_D	45.9	$J_{A,D}$ = 11.7 (11.7)	$J_{B,D}$ = 2.0 (2.1)

2.4 CV measurements

Cyclic voltammetry was performed on a Princeton Applied Research VersaSTAT 3 unit. A three-electrode arrangement with a glassy carbon working electrode, a platinum wire counter electrode and an $Ag/AgBF_4$ in CH_3CN reference electrode and 0.1 M *n*-Bu4NPF$_6$ in CH_2Cl_2 as supporting electrolyte was employed. The ferrocene/ferrocenium (Fc/Fc^+), acetylferrocene/acetylferrocenium ($AcFc/AcFc^+$) or diacetylferrocene/diacetylferrocenium (Ac_2Fc/Ac_2Fc^+) redox couple were used as internal standard. The redox potentials referenced to the ferrocene derivatives have been corrected to reference all redox couples to (Fc/Fc^+). The quasi-reversible character of electron transfer processes have been supported by variation of the scan rates (Figures S22, S23, S24).

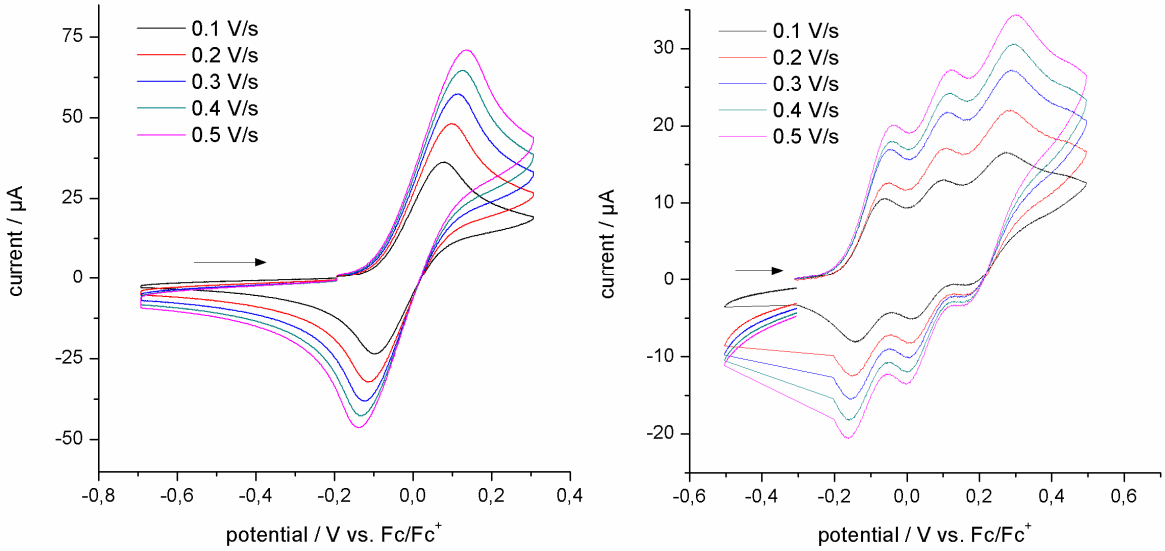

Figure S22. Cyclic voltammograms of **2** (left) and *unlike*-**5** (right) at different scan rates.

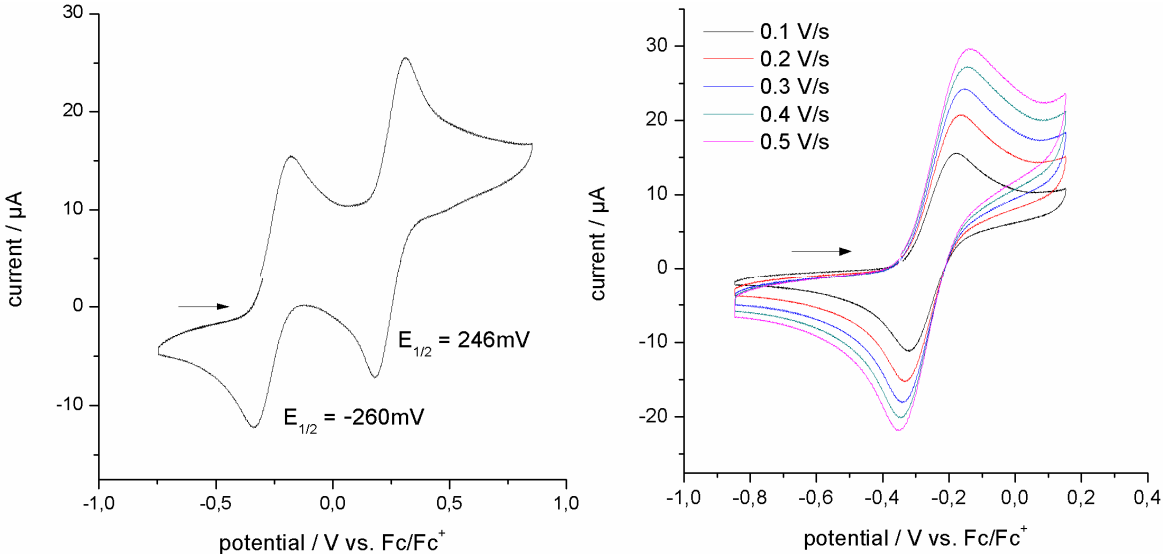

Figure S23. Cyclic voltammograms of **6**-PF_6; scan rate: 0.1 V/s (left); first redox process at different scan rates (right).

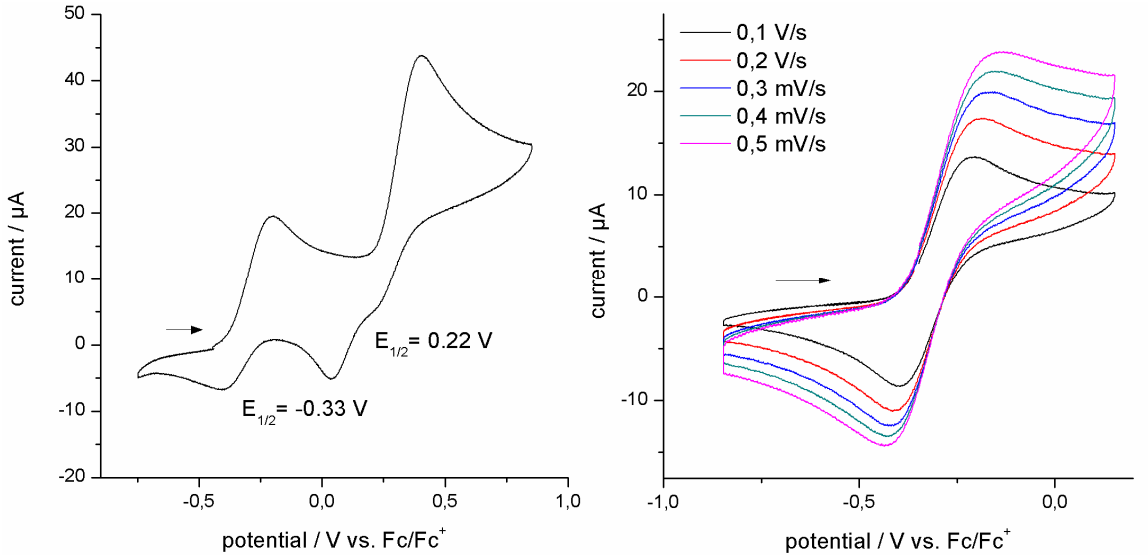

Figure S24. Cyclic voltammograms of **7**; scan rate: 0.1 V/s (left); first redox process at different scan rates (right).

2.4 UV-vis and luminescence measurements

Steady-state UV-vis absorption spectra were recorded with an Agilent 8453 and steady state emission spectra with an Agilent Cary Eclipse spectrometer. The samples were placed in a 1 cm path fused silica cuvette, and dissolved oxygen was removed by bubbling with argon for about 2 min. Corrected emission spectra were obtained via a calibration curve supplied with the instrument. Photoluminescence quantum yields (φ_{PL}) were extracted from corrected spectra on a wavelength scale (nm). A solution of $[Ru(bpy)_3]Cl_2$ (Aldrich) in deaired water (spectrophotometric grade, Alfa Aesar; φ_{PL} = 0.043[12]) or $Ir(ppy)_3$ (Aldrich) in deaired toluene (spectrophotometric grade, Acros Organics; φ_{PL} = 0.73[13]) was applied as standard. Sample and luminescence standard were excited at 450 or 365 nm, respectively, with an absorbance of about 0.1 at the excitation wavelength for both sample and standard.

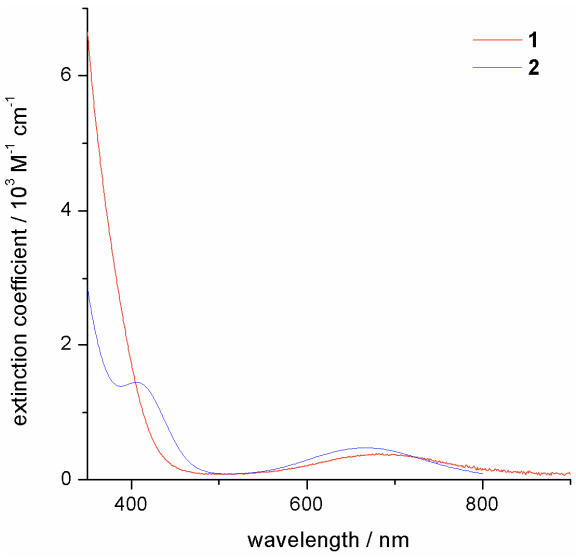

Figure S25. UV-vis spectra of **1** and **2** in CH_2Cl_2.

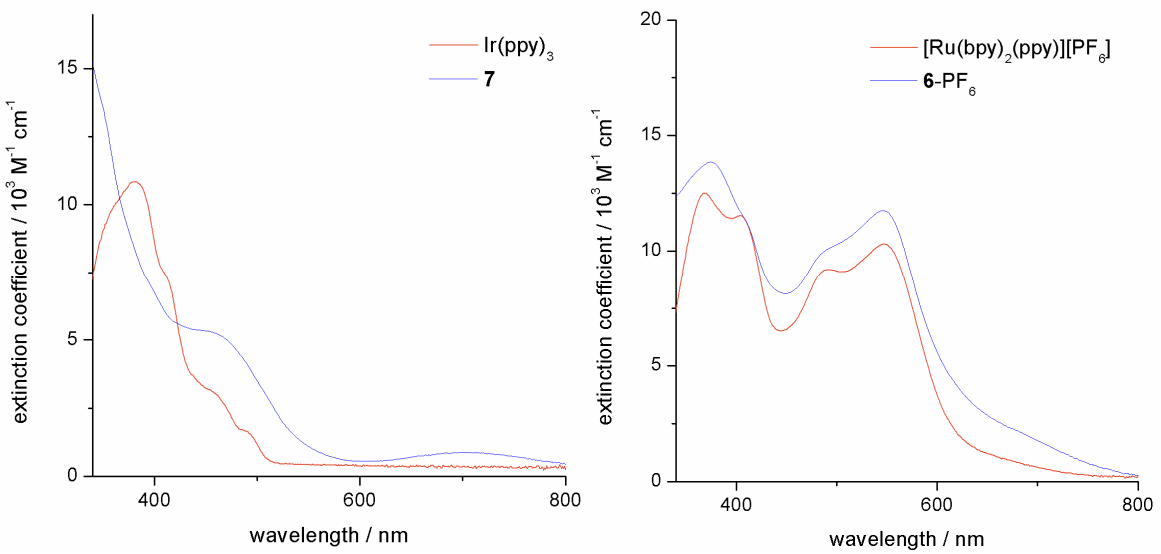

Figure S26. UV-vis spectra of $Ir(ppy)_3$ and **7** in toluene (left) and $[Ru(bpy)_2(ppy)][PF_6]$ and **6**-PF_6 in CH_3CN (right).

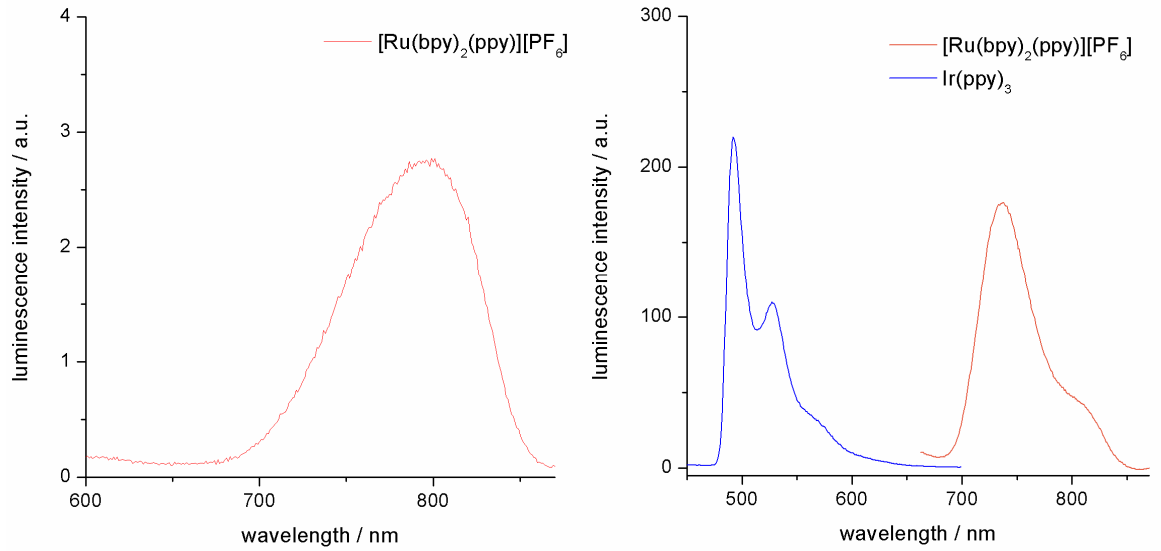

Figure S27. Luminescence spectra of $[Ru(bpy)_2(ppy)]PF_6$ in acetonitrile at 23 °C (left, λ_{exc} = 450 nm) and of $[Ru(bpy)_2(ppy)]PF_6$ (λ_{exc} = 450 nm) and $Ir(ppy)_3$ (λ_{exc} = 365 nm) in butyronitrile at –196 °C (right).

2.5 TD DFT calculations

DFT calculations were carried out as closed shell (S = 0) calculations using the ORCA program package, version 4.1.1.[14] Molecular geometries were optimized without truncation and symmetry constraints in the gas phase using the BP86 functional.[15] Quasi-relativistic effective core potentials were used for W (ECP46MBW) and Ru (ECP28MBW).[16] Split valence triple ζ-basis sets (def2-TZVP) of the Ahlrich group[17] and respective auxiliary basis sets were applied.[18] Dispersion was accounted for by the atom-pairwise dispersion correction with the Becke-Johnson damping scheme (D3BJ).[19] In doing so a reasonable match between the calculated and the experimentally determined structures for **2**, $[Ru(bpy)_2(ppy)]^+$ (for comparison) and $\mathbf{6}^+$ were achieved. Frequency calculations were

performed to identify all stationary points as minima. The Cartesian coordinates are given in Table S7 and S8. TD DFT calculations were performed using the B3LYP functional in combination with split valence triple ζ-basis sets as mentioned above. The range to 380 nm was covered by 10 (**2**), 20 $[Ru(bpy)_2(ppy)]^+$ and 30 (**6**$^+$) calculated singlet/singlet transitions, respectively. Selected states with high oscillator strength are given in Tables S4 to S6 and the difference densities for essential transitions are depicted in Figures S29 to S31. Attempts with higher level functionals like PBE0 (for geometry optimization) or an all electron ZORA approach (TD DFT) did not improve the match of the calculated with experimental data.

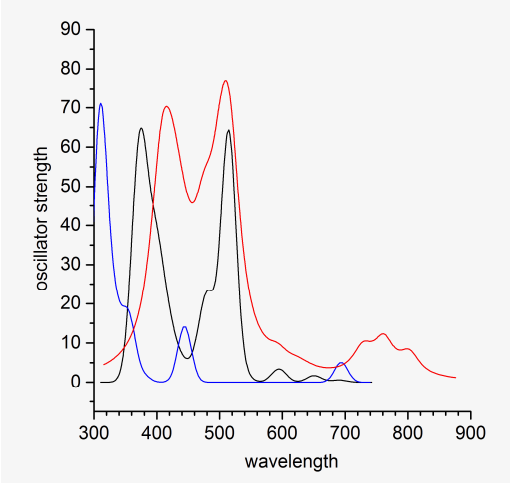

Figure S28. Calculated UV-vis spectra based on TD DFT with $[Ru(bpy)_2(ppy)]^+$ (black), **2** (blue) and **6**-PF_6 (red); Lorentzian line shape and peak width 30 cm^{-1}.

Table S4. Selected singlet/singlet transitions for **2** calculated by TD-DFT.

number	wavelength	oscillator strength	transition character
1	693.6	0.0094	$W(t_{2g}) \leftarrow W(t_{2g})$
2	444.2	0.0265	py-alkyne $\leftarrow W(t_{2g})$
4	355.3	0.0292	py/pyrazole $\leftarrow W(t_{2g})$
9	314.5	0.0287	$W(t_{2g}) \leftarrow$ bromide
10	308.7	0.1007	$W(t_{2g}) \leftarrow$ bromide

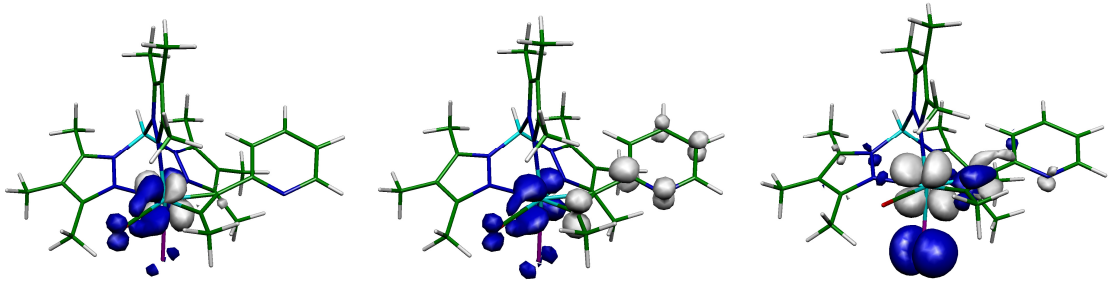

Figure S29. Calculated difference density for transitions 1 (left), 2 (middle) and 10 (right) in **2** (blue=drop, white: gain).

Table S5. Selected singlet/singlet transitions for $[Ru(bpy)_2(ppy)]^+$ calculated by TD-DFT.

number	wavelength	oscillator strength	transition character
5	514.3	0.1326	π^*(bpy) $\leftarrow Ru(t_{2g})$
6	481.8	0.0384	π^*(bpy) $\leftarrow Ru(t_{2g})$
15	396.8	0.0314	π^*(bpy+ppy) $\leftarrow Ru(t_{2g})$
17	380.4	0.0374	π^*(bpy+ppy) $\leftarrow Ru(t_{2g})$
18	372.6	0.0624	π^*(ppy) $\leftarrow Ru(t_{2g})$

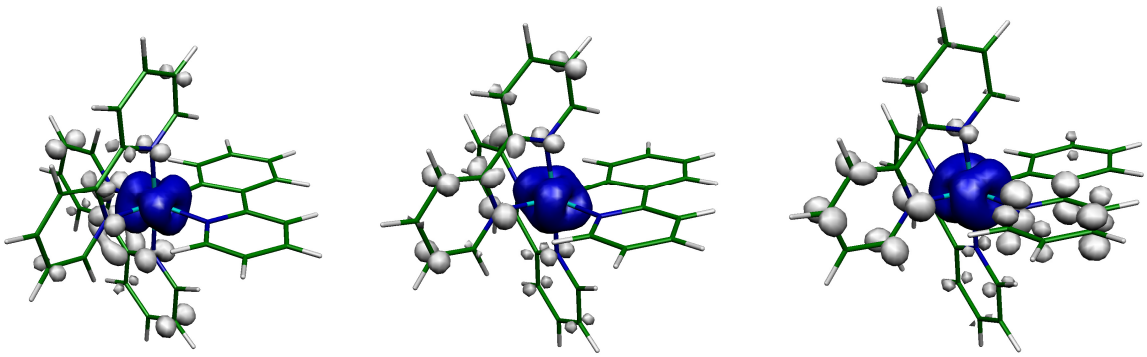

Figure S30. Calculated difference density for transitions 5 (left), 6 (middle) and 18 (right) in $[Ru(bpy)_2(ppy)]^+$ (blue=drop, white: gain).

Table S6. Selected singlet/singlet transitions for $\mathbf{6}^+$ calculated by TD-DFT.

number	wavelength	oscillator strength	transition character
2	802.4	0.0122	bpy ← $W(t_{2g})$: HOMO
3	761.2	0.0188	$W(t_{2g})$ ← $W(t_{2g})$: HOMO
4	728.1	0.0139	bpy ← $Ru(t_{2g})$
9	517.9	0.0495	bpy ← $Ru(t_{2g})$/$W(t_{2g})$: HOMO
10	513.1	0.0278	py-alkyne/bpy ← $W(t_{2g})$: HOMO
11	509.0	0.0269	bpy ← $Ru(t_{2g})$
12	502.0	0.0324	py-alkyne ← $Ru(t_{2g})$
16	472.6	0.0335	bpy ← $Ru(t_{2g})$
27	407.6	0.0618	py-alkyne ← $Ru(t_{2g})$

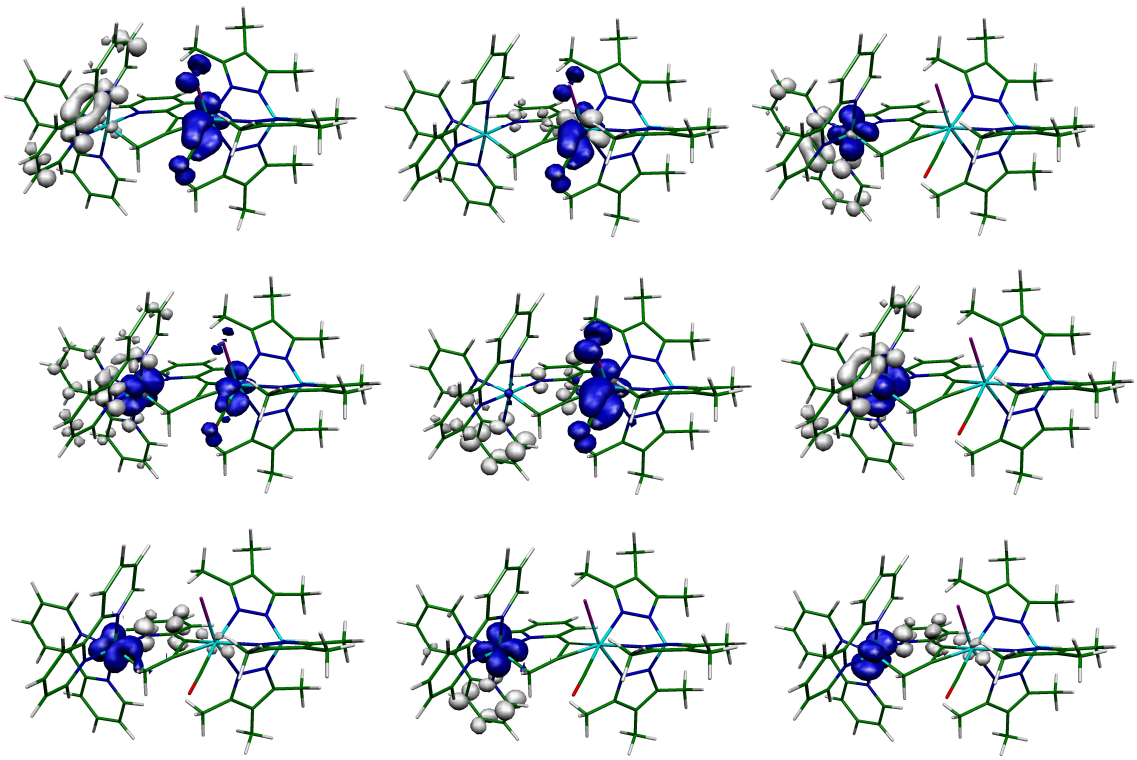

Figure S31. Calculated difference density for transitions in $\mathbf{6}^+$ (blue=drop, white: gain); top row: 2 (left), 3 (middle), 4 (right); middle row: 9 (left), 10 (middle), 11 (right); bottom row: 12 (left), 16 (middle), 27 (right).

2.6 Transient absorption spectroscopy

A setup was used based on a regenerative Ti:Sapphire amplifier system (CPS-2001, Clark MXR) providing ultrashort laser pulses centred at 775 nm with a repetition rate of 1 kHz. Excitation (pump) pulses centred at 720 nm were generated by a noncollinear optical parametric amplifier (NOPA). The dispersion of the NOPA pulses was minimized using a compressor based on fused-silica prisms resulting in a pulse duration of 70 fs. The final wavelength for excitation of 360 nm was reached via frequency doubling using a 0.7 mm thick BBO crystal. Absorption changes were probed over the complete visible spectral range with a white-light continuum generated by focusing a small fraction of the Ti:sapphire output into a rotating CaF_2 substrate. The polarisation of the probe pulses was set to magic angle (~54.7°) relative to that of the pump-pulses. Pump and probe pulses were focused onto the sample to overlap. Their spot diameters were approximately 444 µm for the pump and 133 µm for the probe. After passing through the sample, the probe was spectrally dispersed by a prism, and the TA changes were recorded with a photodiode array detector with 512 pixels. The chirp of the probe signal was corrected numerically in a data processing procedure. The substances were dissolved in CH_2Cl_2 of spectroscopy grade. The solution was measured in a quartz cuvette with a thickness of 1 mm. The obtained data was analyzed using a global fit. In this procedure the multi-exponential model function $F(\lambda, t) = \sum_i^N DAS_i(\lambda) \cdot \exp(-t/\tau_i)$, convoluted with the temporal response of the pump-probe setup, is fitted to the complete set of time dependent transient absorption spectra. In the present case three exponential decay components were necessary, i. e. *N* = 3, to reproduce the data with satisfying accuracy. Thereby, the time constant of the third component was set to infinity, to describe a long living contribution which persists much longer than the experimentally accessible time range.

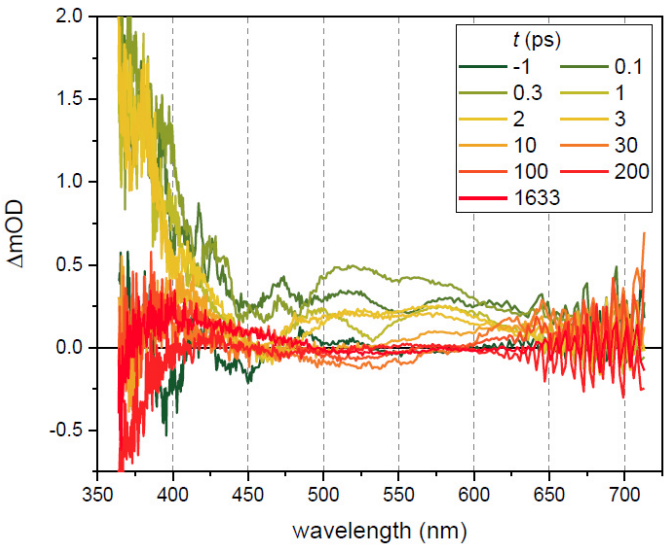

Figure S32. Transient absorption spectra and time traces of **7** in CH_2Cl_2 with magic angle of the probe polarization with respect to the excitation at 360 nm.

2.7 Cartesian coordinates of calculated complexes

Table S7. Cartesian coordinates of the geometry optimized structures of **2** (left) and $[Ru(bpy)_2(ppy)]^+$ (right) in the gas phase; BP86, def2-TZVP/ECP(W,Ru) with empirical dispersion correction (GD3BJ).

W	4.038071	10.851558	13.166906	Ru	-3.067315	-0.013512	0.173068
Br	2.231157	11.311574	11.403929	N	-2.630628	-1.729941	1.157377
N	5.949136	10.419813	14.157178	N	-3.747977	-1.393848	-1.149654
N	5.515824	11.750669	11.748182	N	-5.032082	0.305100	0.925488
N	4.436664	8.995039	11.950611	N	-3.666065	1.657553	-0.856089
C	3.221764	9.509522	14.459485	N	-2.126173	1.243268	1.524492
C	2.848751	10.710620	14.873195	C	-2.035279	-1.808749	2.372346
C	3.790084	12.628912	13.964782	C	-2.926404	-2.899443	0.498584
H	3.565645	13.629913	11.376587	C	-3.562208	-2.709200	-0.800590
H	1.803174	8.720011	12.383438	C	-4.337951	-1.118828	-2.337648
N	6.946127	9.771243	13.477016	C	-5.675896	-0.477925	1.817806
C	6.333756	10.497050	15.453008	C	-5.684066	1.390517	0.412049
N	6.603232	11.019110	11.347824	C	-4.910067	2.162734	-0.564307
C	5.583985	12.949279	11.119171	C	-2.898683	2.317746	-1.758091
N	5.716054	8.678373	11.581453	C	-2.733882	1.843976	2.571866
C	3.645313	7.974334	11.551927	C	-0.791206	1.480400	1.293789
C	3.160066	8.115605	14.839806	C	-1.722839	-3.017246	2.976451
C	2.015500	11.356843	15.903049	C	-2.630427	-4.143260	1.065592
O	3.611359	13.669798	14.477797	C	-3.963886	-3.745049	-1.650789
C	4.582243	14.036137	11.294499	C	-4.753166	-2.108677	-3.215348
C	2.175890	7.890267	11.778432	C	-6.972341	-0.222128	2.244809
B	6.867015	9.624518	11.942638	C	-6.991253	1.701263	0.806986
C	7.953080	9.440677	14.328973	C	-5.377453	3.329985	-1.178269
C	7.591556	9.875441	15.606937	C	-3.320202	3.475541	-2.396719
C	5.516024	11.140173	16.515441	C	-2.067290	2.693912	3.442989
C	7.349311	11.737942	10.472247	C	-0.076976	2.335268	2.146870
C	6.728308	12.979388	10.296932	C	-2.023511	-4.212285	2.314387
C	5.742118	7.470965	10.955056	C	-4.562301	-3.451236	-2.870581
C	4.433620	6.987056	10.919733	C	-7.643924	0.892697	1.731910
N	2.030660	7.685856	15.451839	C	-4.582969	3.997972	-2.103341
C	4.251608	7.263813	14.579160	C	-0.708265	2.944522	3.224051
H	2.465945	12.283026	16.285611	H	-1.808719	-0.857675	2.849318
H	1.804395	10.665104	16.730035	H	-4.457310	-0.062958	-2.571956
H	1.055100	11.641468	15.443062	H	-5.108946	-1.330944	2.191120
H	4.618657	14.718543	10.435227	H	-1.921548	1.876950	-1.948163
H	4.784903	14.626729	12.200271	H	-3.791123	1.617646	2.701324
H	1.637832	7.909976	10.819049	H	-1.241187	-3.016598	3.953420
H	1.926264	6.942814	12.280598	H	-2.871795	-5.055646	0.522932
H	7.903648	9.188148	11.524929	H	-3.802891	-4.780244	-1.354663
C	9.193540	8.751065	13.871026	H	-5.217561	-1.826273	-4.159218
C	8.362529	9.736320	16.881779	H	-7.445347	-0.886447	2.966960
H	5.048817	12.063279	16.151737	H	-7.498025	2.569401	0.389316
H	6.147818	11.380526	17.380225	H	-6.363261	3.716067	-0.925412

H	4.709029	10.477247	16.864000	H	-2.657084	3.960685	-3.111843
C	8.595876	11.202444	9.853518	H	-2.606509	3.149089	4.272299
C	7.164072	14.113097	9.423766	H	0.9792160	2.5166014	1.9544513
C	6.997975	6.865554	10.424425	H	-1.784682	-5.176287	2.761627
C	3.932027	5.698572	10.353015	H	-4.874255	-4.251073	-3.540967
C	1.962083	6.391085	15.784562	H	-8.660964	1.125025	2.046047
H	5.141802	7.662747	14.095693	H	-4.939287	4.908698	-2.583352
C	4.163407	5.926549	14.950426	H	-0.151705	3.607908	3.886142
H	8.969754	7.796480	13.373556	C	-0.250808	0.780409	0.135735
H	9.843845	8.541937	14.729008	C	1.0904961	0.8818468	-0.2747884
H	9.760972	9.365667	13.157077	C	-1.185621	-0.021475	-0.580598
H	9.294952	9.178556	16.724167	C	1.5302645	0.1891235	-1.3984509
H	7.784331	9.200329	17.649572	H	1.7973200	1.5002547	0.2812646
H	8.635066	10.716157	17.304196	C	-0.706428	-0.710971	-1.707833
H	8.404894	10.278268	9.289436	C	0.6274538	-0.6085421	-2.1134928
H	9.360353	10.972994	10.609745	H	2.5695395	0.2662532	-1.7175892
H	9.016667	11.941098	9.160652	H	-1.381252	-1.341247	-2.290903
H	8.044023	13.842438	8.824988	H	0.9701695	-1.1556002	-2.9939881
H	7.427941	15.005653	10.011588				
H	6.369559	14.409248	8.721986				
H	6.772617	5.911790	9.931237				
H	7.730743	6.669102	11.221166				
H	7.485397	7.520508	9.688148				
H	3.240081	5.862512	9.512087				
H	3.384961	5.115183	11.110103				
H	4.755488	5.072020	9.984974				
C	2.990074	5.470865	15.556495				
H	1.032258	6.071246	16.264830				
H	4.994468	5.245707	14.760109				
H	2.871441	4.428151	15.852594				

Table S8. Cartesian coordinates of the geometry optimized structures of $\mathbf{6}^{+}$ in the gas phase; BP86, def2-TZVP/ECP(W,Ru) with empirical dispersion correction (GD3BJ).

Ru	-3.095384	0.06652	-0.06018	C	6.0521634	-0.8949153	-0.9582513
N	-2.521402	-1.66151	0.81039	C	4.3201165	-2.1421831	-1.6274956
N	-4.066990	-1.27893	-1.22020	C	5.7258194	-2.0638428	-1.6550380
N	-4.893576	0.34229	1.01189	C	7.3891390	-0.2982153	-0.6770013
N	-3.853683	1.77311	-0.91350	C	3.4840737	-3.2061259	-2.2467456
N	-1.950280	1.36852	1.18668	C	6.6566033	-3.0381438	-2.3044809
C	-1.519582	-0.26856	-1.45332	H	-1.573115	-1.273558	-1.909609
C	-1.837394	-1.76866	1.97218	H	-1.608134	0.428264	-2.304946
C	-2.866583	-2.81322	0.14532	H	-1.602824	-0.829146	2.466035
C	-3.729324	-2.59348	-1.01035	H	-5.160307	0.076451	-2.343870
C	-4.931240	-0.97976	-2.21584	H	-4.674599	-1.241928	2.328918
C	-5.379626	-0.50217	1.94956	H	-2.199019	2.234635	-2.069024
C	-5.728026	1.30095	0.50098	H	-3.701416	2.142733	1.984746

C	-5.102756	2.17246	-0.49426	H	-0.864535	-3.012091	3.418451
C	-3.190247	2.57526	-1.78019	H	-2.735244	-4.964238	0.062995
C	-2.617366	2.22309	2.00085	H	-3.948502	-4.638728	-1.658233
C	-0.568303	1.43445	1.19826	H	-6.162761	-1.647926	-3.839366
C	-0.251929	-0.08771	-0.77216	H	-7.026659	-1.150131	3.164674
C	-1.434868	-2.98959	2.49190	H	-7.713636	2.154730	0.479122
C	-2.469343	-4.06711	0.61934	H	-6.675324	3.641723	-0.622602
C	-4.242012	-3.60460	-1.83033	H	-3.135264	4.349305	-2.980093
C	-5.477370	-1.94681	-3.04753	H	-2.610202	3.803144	3.447553
C	-6.688893	-0.44434	2.40668	H	1.1952350	2.3589035	1.9826880
C	-7.060595	1.40201	0.91832	H	-1.411797	-5.133202	2.168737
C	-5.689010	3.34785	-0.97820	H	-5.517429	-4.066345	-3.507801
C	-3.723434	3.75192	-2.28467	H	-8.587272	0.589020	2.209844
C	-1.997934	3.15226	2.82484	H	-5.452412	5.065234	-2.264754
C	0.1513239	0.567779	0.323502	H	-0.080252	3.945216	3.468099
C	0.1069370	2.357629	2.018148	H	2.6427559	-3.4853139	-1.6004128
W	1.7577691	-0.460168	-0.377641	H	5.7215135	1.5748348	0.3453426
C	-1.741482	-4.16385	1.79859	H	0.6313695	2.9627053	-3.4732338
C	-5.119146	-3.28600	-2.86037	H	-0.075920	2.396227	-1.942252
C	-7.551053	0.52449	1.87995	H	0.5761991	1.2194864	-3.1002745
C	-5.004714	4.14700	-1.88653	H	1.3995453	-1.3360849	4.0973376
C	-0.600249	3.22676	2.83421	H	0.5187021	0.1861958	3.8528765
Br	1.4803520	-2.777865	0.693456	H	5.3090141	4.7794437	-1.6245308
N	3.8245294	-1.081522	-0.937902	H	6.1853161	3.2624058	-1.3300302
N	2.5662832	1.415642	-1.174839	H	5.4047444	4.1083384	0.0154847
N	2.7652088	0.147092	1.551802	H	3.6793183	5.2569609	-3.0024329
C	1.1804438	-1.137957	-2.133926	H	1.9770594	5.3210497	-2.5221298
N	3.7770431	1.889611	-0.742448	H	2.4591741	4.4260192	-3.9748188
C	2.0566313	2.346073	-2.018988	H	5.7583806	2.0462876	4.1022265
N	3.9681832	0.798907	1.507928	H	6.5225287	1.2613215	2.7057015
C	2.4102730	0.074238	2.855662	H	5.7017034	2.8175170	2.5027829
O	0.7831651	-1.517333	-3.169208	H	2.4342560	1.2862544	5.4944234
B	4.6733805	1.023400	0.164183	H	3.4318174	-0.1693279	5.6321907
C	4.0375858	3.096764	-1.308559	H	4.2010912	1.4223589	5.5156499
C	2.9507742	3.429776	-2.123954	H	8.1807995	-0.9768330	-1.0152283
C	0.7288466	2.218180	-2.673277	H	7.5331827	-0.1133131	0.3961484
C	4.3716524	1.140148	2.760491	H	7.5236086	0.6610306	-1.1979730
C	3.3936634	0.695662	3.653578	H	4.0978078	-4.0979121	-2.4267522
C	1.1612085	-0.558541	3.356301	H	3.0747339	-2.8827866	-3.2148740
N	4.8959458	-0.324658	-0.537197	H	7.7018086	-2.8295096	-2.0428674
C	5.2991528	3.847395	-1.047354	H	6.5800189	-3.0082926	-3.4021565
C	2.7563478	4.666494	-2.943227	H	6.4411156	-4.0701270	-1.9905964
C	5.6540996	1.853154	3.027898	H	0.6111579	-1.0283227	2.5382932
C	3.3656929	0.815513	5.143710				

3. References

1 G. M. Sheldrick, *SHELXS-2013. Program for Solution of Crystal Structure*, Univ. Göttingen, 2013.
2 G. M. Sheldrick, *SHELXS-2013. Program for Refinement of Crystal Structure*, Univ. Göttingen, 2013.
3 P. H. M. Budzelaar, *gNMR for Windows*, IvorySoft, 2006.
4 K. Helmdach, S. Ludwig, A. Villinger, D. Hollmann, J. Kösters and W. W. Seidel, *Chem. Commun.*, 2017, **53**, 5894–5897.
5 N. G. Connelly and W. E. Geiger, *Chem. Rev.*, 1996, **96**, 877–910.
6 M. R. R. Prabhath, J. Romanova, R. J. Curry, S. R. P. Silva and P. D. Jarowski, *Angew. Chem. Int. Ed.*, 2015, **54**, 7949–7953.
7 Z. Chen, Y. Xiong, R. Etchenique and S. Wu, *Chem. Commun.*, 2016, **52**, 13959–13962.
8 N. A. Carmo Dos Santos, M. Natali, E. Badetti, K. Wurst, G. Licini and C. Zonta, *Dalton Trans.*, 2017, **46**, 16455–16464.
9 M. Al-Noaimi, I. Warad, O. S. Abdel-Rahman, F. F. Awwadi, S. F. Haddad and T. B. Hadda, *Polyhedron*, 2013, 110–119.
10 P. G. Bomben, K. C. D. Robson, P. A. Sedach and C. P. Berlinguette, *Inorg. Chem.*, 2009, **48**, 9631–9643.
11 Z.-F. Zhu, J.-L. Tu and F. Liu, *Chem. Commun.*, 2019, **55**, 11478–11481.
12 K. Suzuki, A. Kobayashi, S. Kaneko, K. Takehira, T. Yoshihara, H. Ishida, Y. Shiina, S. Oishi and S. Tobita, *Phys. Chem. Chem. Phys.*, 2009, **11**, 9850–9860.
13 W. Holzer, A. Penzkofer and T. Tsuboi, *Chem. Phys.*, 2005, **308**, 93–102.
14 a) F. Neese, *Software update: the ORCA program system, version 4.0*, Wiley Interdisciplinary Reviews: Computational Molecular Science 2017, **8**, e1327.; b) F. Neese, *The ORCA program system, Wiley Interdiscip. Rev.: Comput. Mol. Sci.*, Wiley Interdiscip. Rev.: Comput. Mol. Sci., 2012, **2**, 73-78.
15 a) Perdew, *Phys. Rev. B*, 1986, **33**, 8822–8824; b) A. D. Becke, *J. Chem. Phys.*, 1986, **84**, 4524–4529.
16 D. Andrae, U. Haeussermann, M. Dolg, H. Stoll and H. Preu, *Theoret. Chim. Acta*, 1990, **77**, 123–141.
17 F. Weigend and R. Ahlrichs, *Phys. Chem. Chem. Phys.*, 2005, **7**, 3297–3305.
18 F. Weigend, *Phys. Chem. Chem. Phys.*, 2006, **8**, 1057–1065.
19 a) S. Grimme, S. Ehrlich and L. Goerigk, *J. Comput. Chem.*, 2011, **32**, 1456–1465; b) S. Grimme, J. Antony, S. Ehrlich and H. Krieg, *J. Chem. Phys.*, 2010, **132**, 154104.